AN ABSTRACT OF THE THESIS OF

CLIVE EDGAR DORMAN (Name) for the MASTER OF SCIENCE (Degree)

in OCEANOGRAPHY (Major) presented on June 22, 1971 (Date)

Title: MOTIONS OF A SMALL SPAR BUOY

Redacted for Privacy

Abstract approved: _____

Dr. Stephen Pond

The motions of a small spar buoy were measured in deep water. The measured variables were two buoy tilts, three accelerations, two wave slopes and the wave height. The variables were corrected for buoy motion and rotated to stationary coordinates, Fast Fourier Transformed, and analyzed spectrally. Analysis included power spectra, coherence, phase and transfer functions. It was found that the buoy was a surface follower at low frequencies up to the frequency of the peak of the wave spectrum. At higher sea wave frequencies, the buoy resists sea motion. The RMS tilts of the buoy are about 0.6 of the RMS sea slopes, and practically all of the buoy motion is concentrated in the frequency band from 0.1 to 0.3 Hertz.

Motions of a Small Spar Buoy

by

Clive Edgar Dorman

A THESIS

submitted to

Oregon State University

in partial fulfillment of
the requirements for the
degree of

Master of Science

June 1972

APPROVED:

Redacted for Privacy

Associate Professor of Oceanography
in charge of major

Redacted for Privacy

Chairman of Department of Oceanography

Redacted for Privacy

Dean of Graduate School

Date thesis is presented June 22, 1971

Typed by Mary Jo Stratton for Clive Edgar Dorman

ACKNOWLEGEMENTS

I am deeply indebted to Dr. G. Stephen Pond, my major professor, for providing the means to carry out this investigation and guidance throughout the project. The aid of Dr. Marshal Earle in his collection of the wave data was indispensible. I am also grateful to Dr. G. Thomas Phelps and Dr. J. Paquin for their programming assistance.

This work was supported by the Office of Naval Research under contract N000 1 4-67-A-9369-007. In addition, my studies were further made possible by financial support from the Veterans Administration's Educational Assistance.

TABLE OF CONTENTS

LIST OF TABLES

LIST OF FIGURES

MOTIONS OF A SMALL SPAR BUOY

I. INTRODUCTION

Increasingly large numbers of air-sea measurements are being made from buoys. While it is apparent that the motion of the buoys affects the air-sea measurements, the extent of the effects is not known. It is the purpose of this investigation to measure the motion of a small spar buoy at sea. With this information, other investigators may make better estimates of the errors in air-sea measurements caused by buoy motions.

Background

Two important air-sea measurements that are made from buoys are the turbulent Reynolds stress and the wind speed gradient. From theoretical considerations, Pond (1968) has investigated the effect of buoy motion on the measurements of the Reynolds stress at sea. He found that certain aspects of buoy motion, particularly the tilting, may lead to significant errors in these measurements.

Let us first consider the general nature of energy contained in the surface waves of the ocean. The energy of the ocean is predominantly peaked at about 0.1 cycles per second (Kinsman, 1965). There is very little relative energy associated with wave frequencies greater than about 1.0 cycles per second or less than about 0.05 cycles per

second. Thus, any floating object on the sea surface will tend to be driven by waves predominantly around 0.1 cycles per second.

Most of the waves that account for the major portion of the total wave energy adhere very closely to the first order small amplitude wave theory. From this theory we know that in deep water, as a wave passes, the water particles move around in circular orbits. An object, such as a buoy floating on the surface, will tend to have the same motions as the water particles would have had if the buoy were not there. Thus, for waves much longer than the size of the buoy, the buoy will move in an approximately circular motion about a stationary point.

In addition to circular orbits, small amplitude first order wave theory for deep water predicts that velocities and pressures will be proportional to:

$$A \exp\left(-\frac{2\pi Z}{L}\right)$$

where

A = amplitude of the wave

L = the wave length

Z = depth.

Thus the velocity and pressure due to a passing wave are greater at any depth for larger wave lengths for a given amplitude. The effect of the pressure and velocity of a passing wave also decreases

exponentially with depth. The result is that a spar buoy will experience a decreasing force along its length.

Now that we have considered something about the forces exerted by ocean waves, we should consider how they act on a floating buoy. Since buoys are usually symmetrical about the vertical axis, the possible forces and torques are simplified. Usually horizontal forces result in a horizontal center of mass acceleration of the buoy and may produce a rotational acceleration in the plane of the force and the vertical. Vertical forces usually produce only vertical accelerations of the center of mass since there is little coupling between the vertical forces and movements other than vertical.

A small flat buoy was used by Longuet Higgins et al. (1963) to study wave spectra. The buoy was 5 feet 6 inches in diameter and about a foot thick. To a first approximation, this buoy may be regarded as moving in small oscillations about a fixed point. For waves sufficiently long compared with its diameter, the buoy will tend to have the same vertical and horizontal displacements as a particle in a free wave, and hence take up the same orientation as the free surface. The buoy motion may be described by:

$$\eta, \frac{\partial \eta}{\partial x}, \frac{\partial \eta}{\partial y}$$

η = the vertical displacement of the sea surface

$\frac{\partial \eta}{\partial x}, \frac{\partial \eta}{\partial y}$ = the slopes of the surface in two perpendicular directions.

It should be noted that due to the low flat profile, the coupling between the pitch and roll and the horizontal displacements (the surge and sway) is negligible. Thus, a force on the side of the buoy parallel to the surface will not cause the buoy to tilt with respect to the surface.

This flat buoy was measured for frequency response. It was found to have a heave and pitch resonance frequency of 4.0 radians per second. Because of high damping, the amplitude response factor of the buoy did not differ appreciably from unity whenever the wave frequencies were less than or equal to 3.5 radians per second. Because of the size and geometry of this flat buoy, it is a very good surface follower for deep water waves with a frequency of less than about 0.5 cycles per second. It was for this reason that Longuet Higgins et al. decided to use the flat buoy to directly measure wave spectra. They made measurements by simply placing a gyroscope and an accelerometer on the buoy.

After considering one of the smallest instrumented buoys let us go to the other end of the buoy spectrum and consider the result of wave action on the largest buoy, FLIP (Floating Instrument Platform, Bronson and Glosten, 1968). FLIP is interesting to study not only because of its large size but also because of its geometry (Rudnick, 1964, 1967). FLIP extends to a depth of 300 feet below the water line when in vertical position. Below the water line, the hull consists first of a smaller cylinder of 12.5 feet in diameter, then expands to a

larger cylinder 20.0 feet in diameter. Depth from the water line to the top of the flair is 60 feet; while the depth to the bottom of the flair is 150 feet. FLIP displaces 2, 104 tons and is indeed a large spar buoy.

FLIP may be approximated by a simple cylinder floating vertically and supported by bottom pressure. The bottom will experience variation in pressure due to wave pressure only to the extent that wave action penetrates to the depth of the bottom of the buoy. For a cylinder of 91 meter draft, Rudnick calculated that the heave frequency would be 0.052 cycles per second (19.2 second period). There still may be appreciable energy in long period swell of this frequency and so the buoy would amplify the energy input of the sea surface. It was thought that the heave resonance needed to be reduced to a point well below any natural long period swell with any appreciable energy. In order to reduce the vertical resonance frequency, the cross section was reduced at the water line, which reduced the restoring force and resulted in a heave frequency of 0.037 cycles per second (27 second period). This reduction is due to the shoulder at intermediate depths feeling the downward wave pressure. The waves of higher frequency will act predominately upon the shoulder rather than on the bottom of the buoy. The shoulder has a lesser cross sectional area than the bottom of the buoy, but is closer to the surface. The average diameter of the shoulder at 32 meters depth is 61% of that of the bottom.

Because of the "shoulder effect" there is a critical wave frequency at which attenuation with depth just offsets the area/depth ratio between the shoulder and the bottom. The result is that the longer swell generates upward forces on the bottom while the shorter waves generate a downward force on the shallower shoulder. The null frequency for FLIP was found to be 0.046 cycles per second (21.6 second period). The result of the shoulder on FLIP is a substantial attenuation in its vertical motion.

There is much less attenuation of motion in the horizontal direction than in the vertical. The surface motion of the water affects the buoy directly. The horizontal forces on the buoy are due to the horizontal pressure of the water against the side of FLIP as a wave passes. The effect decays exponentially with depth. So, reduction of the hull cross section in the wave zone and the expansion of the hull in the quieter region below is helpful.

Because of the shape, FLIP has a natural roll frequency of 0.021 cycles per second. Under average sea conditions the typical RMS angular displacement would be of the order of 0.25 degrees. The typical median RMS values of vertical and horizontal accelerations would be about 1 cm/sec^2 and 20 cm/sec^2, respectively.

Now that we have considered the extremes of buoy size--from the very large to the very small-let us compare those buoys to the buoy used in this investigation. The spar buoy utilized in this investigation

has a sub-surface length of 24 feet (7.32 m); a water-line diameter of 4 feet (1.22 m); and a mass of 1,200 lbs (546 kgm). The buoy is a small spar buoy and is in between the sea-surface response characteristics of the small Longuet-Higgins buoy and the large spar buoy, FLIP. However, it is much more like the latter, in that it will tend to resist pitch and roll forces and be more stable than the small Longuet-Higgins buoy.

The smaller size of the buoy used in this study leads to many advantages. The principle advantage is in ease of handling and maneuverability. It can be easily kept in dry storage when not in use. Maintenance and upkeep are minimal. It is, therefore, a cheap buoy to build, use and maintain. In addition to the advantages of a small buoy, we will show that this buoy also incorporates some of the stability and response characteristics of a larger one.

Statement of the Problem

The problem is to relate the center of drag response of a small spar buoy to the driving force of the sea. To determine the motion of the buoy, an accelerometer and a gyroscope are used to measure three linear accelerations and two tilts of the buoy. These accelerations must be corrected for buoy motion and rotated to a stationary coordinate system; the tilts are measured with reference to a stationary coordinate system.

The motion of the sea, which principally drives the buoy, is determined from two wave slopes and a wave height. These variables also must be corrected for buoy motion and rotated to a stationary coordinate system.

Thus, eight variables are used: three linear accelerations, two tilts, two wave slopes, and a wave height. Once corrections and rotations are made, the variables are Fast Fourier Transformed and analysed spectrally to find the buoy response to the sea. Analyses include power spectra, cross-spectra, coherences, phases and transfer functions, among the driving forces (slopes and height) and the responses (accelerations and tilts).

II. EQUIPMENT AND DATA ACQUISITION

Equipment

The principal piece of equipment used in this experiment, the small spar buoy, can be seen in Figures 1, 2, and 3. Basically, the buoy is a triangular television tower 15 m long with a weighted foot and six fiberglass toroids around the center to provide buoyancy. The toroids have an outer radius of 2 feet (0.61 m); an inner radius of 1 foot (.61 m), and a thickness of 1 foot (.31 m). The overall mass of buoy is 546 kgm. Wave poles and buoy motion instruments were attached to the structure of the buoy. The motion instruments consisted of a vertical gyroscope and a linear accelerometer.

The gyroscope used was a Humphrey Inc. Vertical Gyroscope model V624-0801-1. This gyroscope measures pitch angles of $\pm 60^{\circ}$ and roll angles of $\pm 90^{\circ}$. Static error band of the pitch is 1.25% of full scale at 0°, that of roll is $\pm$ 0.83% of full scale at 0°.

The linear accelerometer was also made by Humphrey Inc. It is a three-axis linear accelerometer model number LA73-0101-1. Its range for the X and Y axis is $\pm$ 1 g, while the range in the Z axis is $\pm$ 1 g about a +1 g bias so that the output is zero when the instrument is stationary in the earth's gravitational field. The accuracy is $\pm$ 1% of full scale.

The three wave poles were constructed at OSU. Each pole is 20

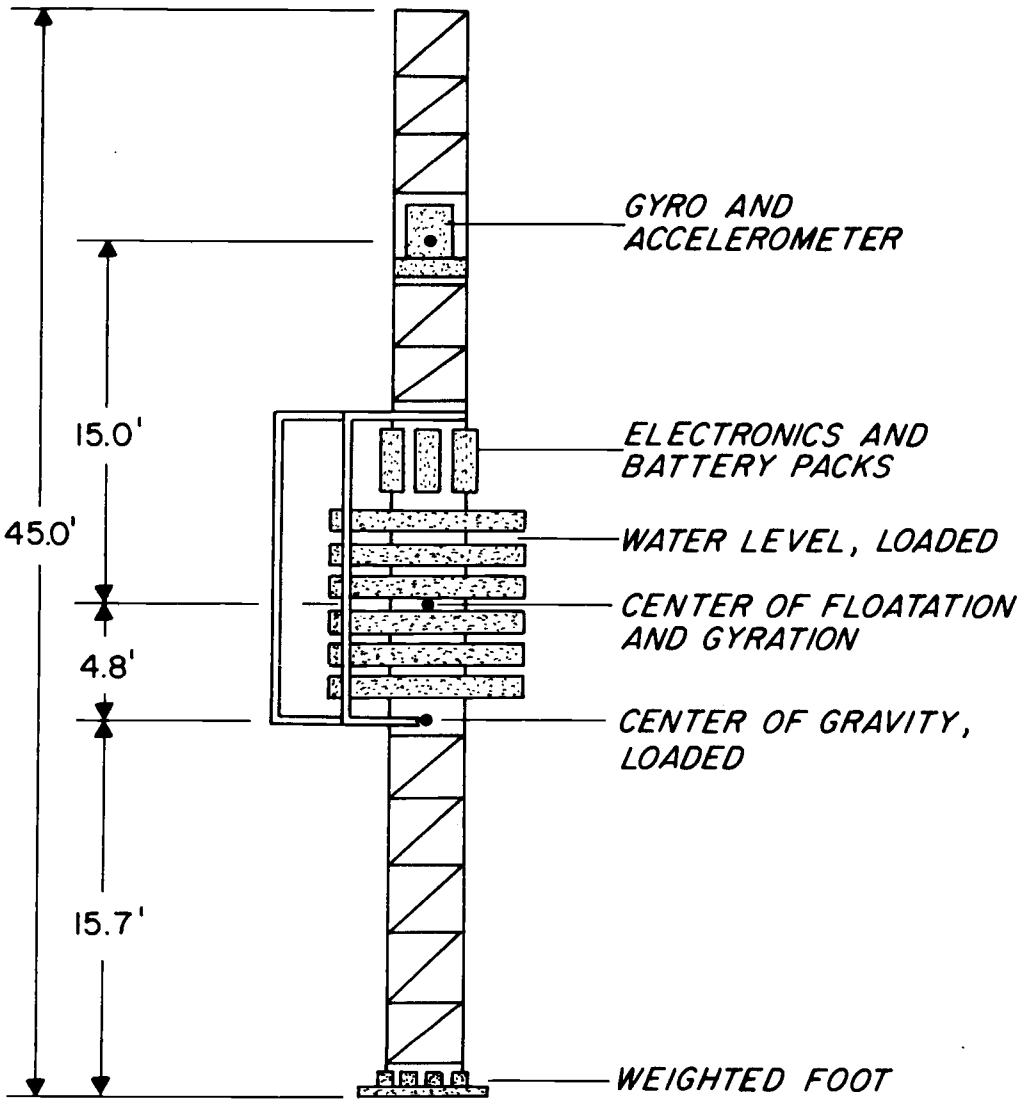

Figure 1. Buoy -- side view.

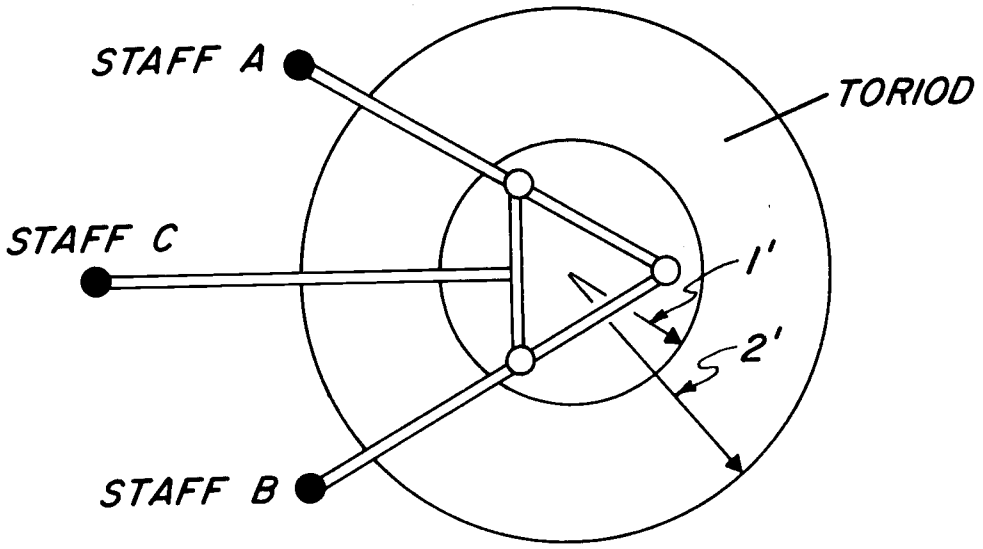

Figure 2. Buoy -- top view.

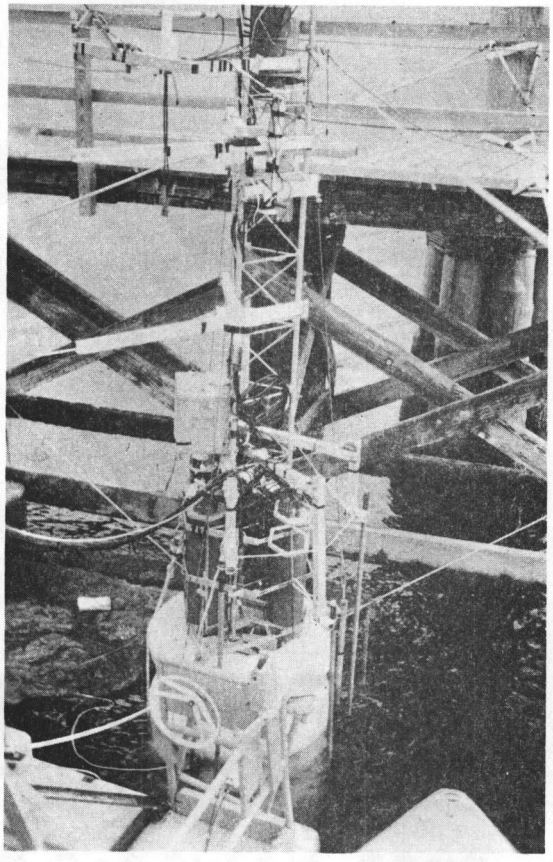

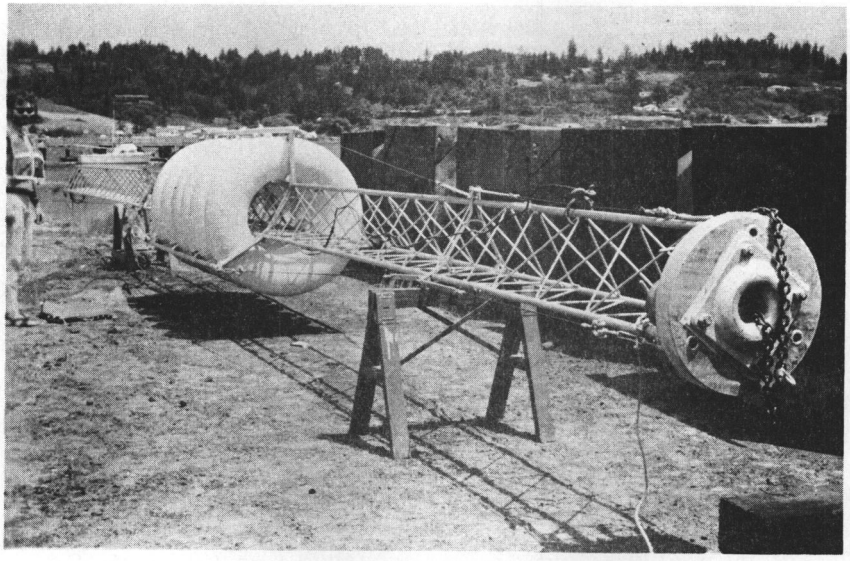

Figure 3. Photographs of the buoy.

feet long, 1 inch diameter P. V. C. that has been threaded. NiCr wire was wound in the threads of the poles to provide the resistance path. The resistance of the poles was found to be 3.79 ohms per cm.

The placement of the wave poles and the motion instruments can be seen in Figure 1. The accelerometer and gyroscope were placed inside the tower about 3 m above the water line. The axes of both of these instruments were aligned. The arrangement of the wave poles is shown in Figure 2. The poles are arranged in a right angle and project halfway out of the water. The axes of the gyro-acceleration system were parallel and perpendicular to the support of staff C. Thus the wave pole axes are rotated 45° from the gyro-acceleration axis.

The three acceleration signals were put into voltage controlled oscillators with different center frequencies and multiplexed together for transmission by cable to the ship. The two tilt signals were treated in the same fashion as the acceleration signals. The wave height and wave slope signals were transmitted directly over the sea cable to the ship. The signals were then recorded on an analogue magnetic tape recorder (Hewlett Packard System 3955). A schematic diagram of the data collection system is shown in Figure 4.

Later the analogue tape data was converted to digital form. The analogue signals were reproduced with the same tape recorder system that was used to collect the data. Then the signals were separated by Sonex discriminators. At this point, all eight channels were passed

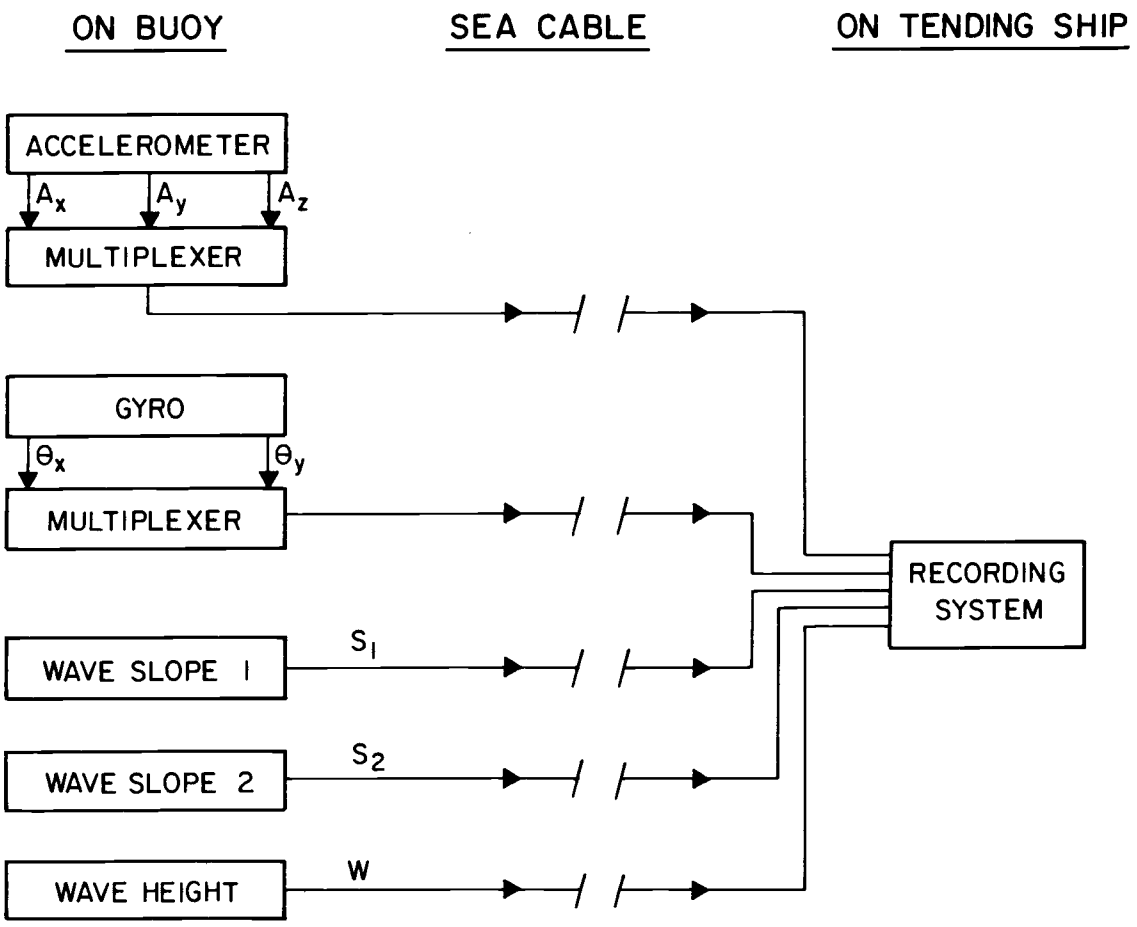

Figure 4. Data acquisition system.

through filter/amplifiers and then to an Analogue-to-Digital convertor. Figure 5 shows a block diagram of the signal processing system.

The filter/amplifiers that were used were made to remove high frequency noise and to improve the digital resolution. They had the characteristics of a double RC roll off, low pass filter which was three db down at 5.9 Hz. The filter components were matched so that the phase between channels would be preserved. This filtering removes any noise above the band of interest. The filter cut-off is high enough that neither amplitude or phase are affected in the frequency band of interest. The analogue-to-digital convertor had an input range of $\pm$ 10 volts with corresponding output of $\pm$ 8192. The signals from the tape recorder and Sonex discriminators were typically smaller than $\pm$ 10 volts (of order $\pm$ 1 volt). Thus amplification was provided to insure good digital resolution so that digital resolution noise is negligible. A sample of the signals at the outputs of the filter/amplifiers is shown in Figure 6.

The digitizing was done on an EAI computer, operated by the Department of Electrical Engineering at OSU under the direction of Dr. John L. Saugen. The digitizing rate was 8.333 Hz. The digitized data were then in a form to be accepted by the CDC 3300 computer where the actual data processing was done.

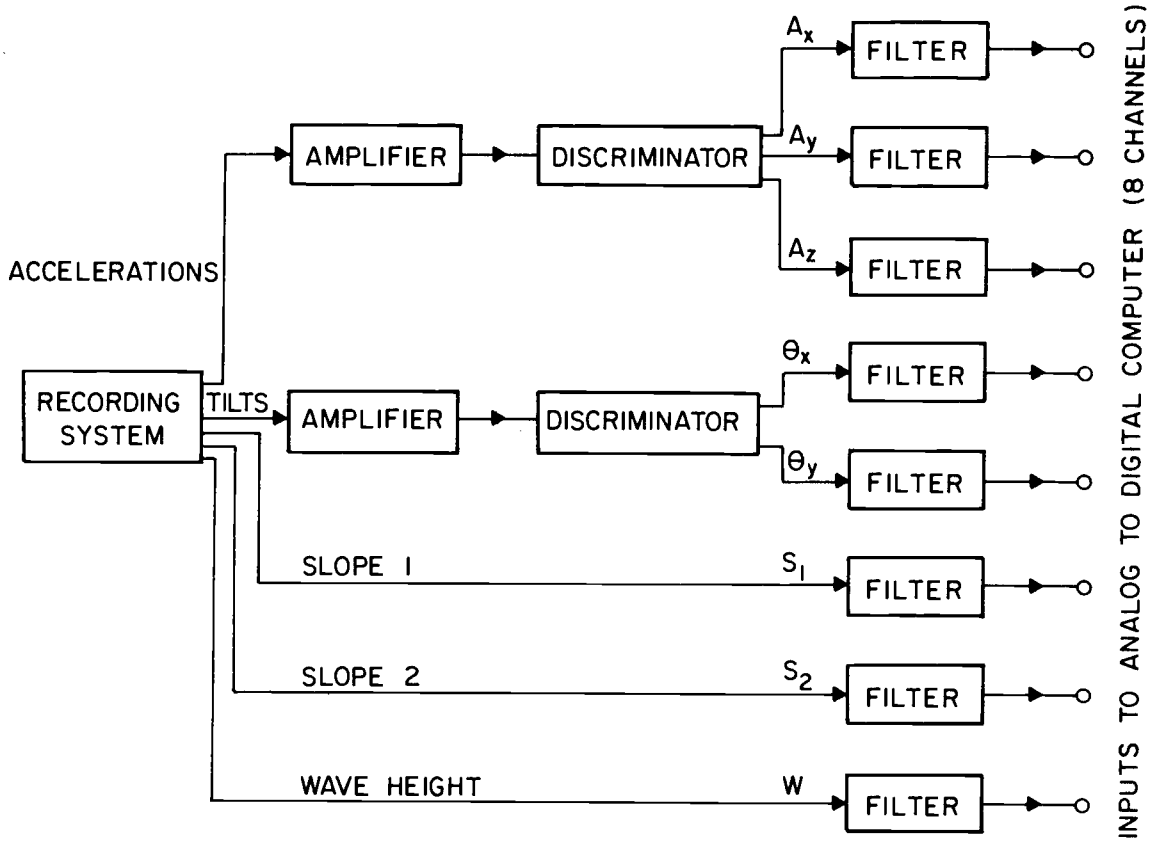

Figure 5. Analogue to digital conversion system.

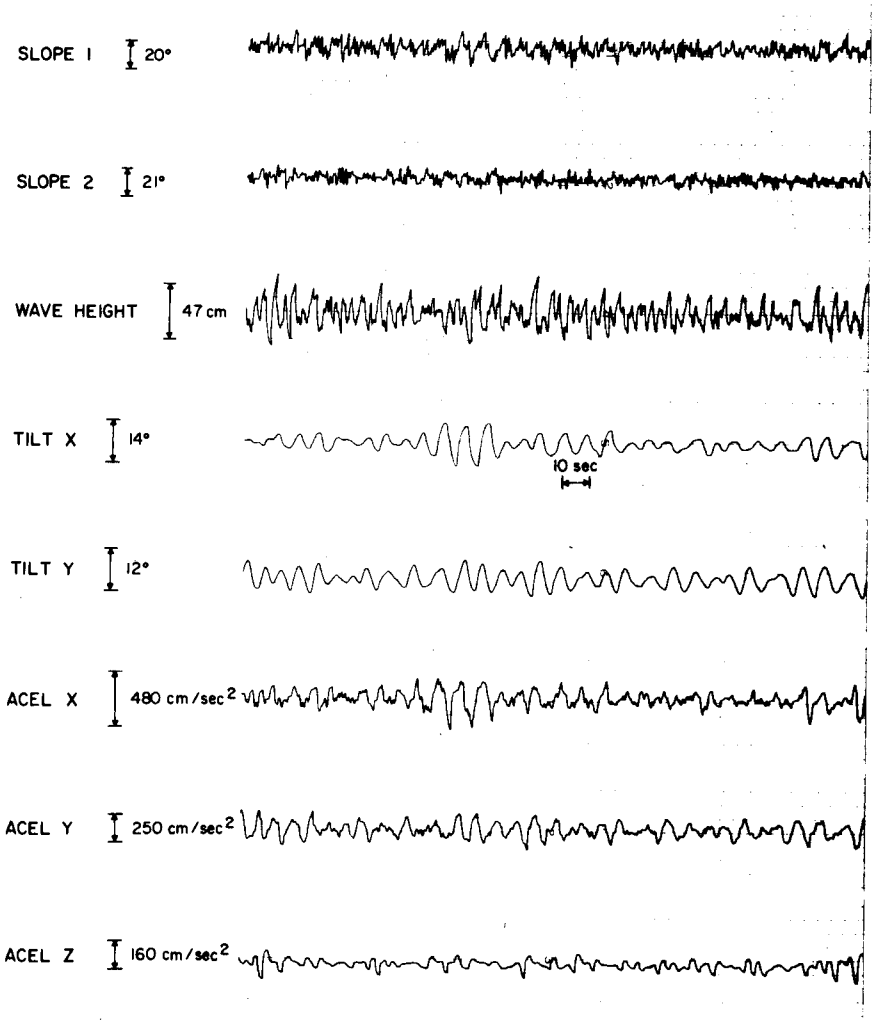

Figure 6. Sample of signals from recording system.

Data Acquisition

The actual data came from two cruises, each about 5 miles off Newport, Oregon, in 60 m of water. One cruise was in September, 1969; it will be called Record 1. Records 2 and 3 came from a cruise in August, 1969. Record 1 was 30 minutes long while Records 2 and 3 were each 15 minutes long. In all records the waves were coming from off-shore and should be typical of open ocean conditions.

III. COMPUTATIONS

Time Series

In this work, time series techniques are used extensively. Let us briefly review time series analysis. Blackman and Tukey (1958), Jenkins and Watts (1968) and Lathi (1968) are good references on time series. We know from them, for example, that a variable that is a function of time, and therefore in the time domain, is equivalent to a distribution of amplitudes in the frequency domain. The time domain and the frequency domain representations are equivalent and a variable in one domain may be transferred to the other domain.

For analysis, it is necessary to have the time domain function digitized. Digitizing takes samples of an analogue signal at regular intervals, Δt, for some length of time T, for a total of n numbers. The time domain digitized function can be converted to a Fourier series, resulting in a frequency domain representation. The minimum frequency will be $1/T$ (where T is the maximum period). The maximum frequency will be $1/(2\Delta t)$ (minimum period), which is also known as the Nyquist frequency. The Fourier series is a frequency domain representation with two numbers for each frequency, which may be thought of as a complex number or vector. Thus, a function A may be represented in the frequency domain as:

$$A - \bar{A} = \sum_{i=1}^{n/2} a_i \cos(2\pi f_i t) + b_i \sin(2\pi f_i t)$$

where $\bar{A}$ is the mean, and $f_i = i/T$. If we transformed n numbers of a variable to the frequency domain, we would have n Fourier coefficients, but only n/2 frequencies.

Modern time series analysis uses the Fast Fourier Transform. The Fast Fourier Transform yields the same results as the Fourier series analysis, but with a greatly reduced number of computations. A reduction in the number of computations means a significant reduction in necessary computer time and expenses.

There are many advantages to dealing with a variable in the frequency domain. Integration in the time domain is equivalent to dividing the Fourier coefficients by $2\pi f_i$ and changing cosine to sine and sine to -cosine in the frequency domain. Differentiation in the time domain is equivalent to multiplying the Fourier coefficients by $2\pi f_i$, changing cosine to -sine and sine to cosine in the frequency domain. Filtering may be performed by transforming to the frequency domain, and setting all of the undesired frequency's coefficients to zero; then inverse Fourier transforming back to the time domain.

Fourier series may be extended to spectral analysis. A function in the frequency domain may be arranged in terms of its autospectra. An autospectra, ϕ, can be obtained from a Fourier series. As an example, for the function A, for a frequency i,

$$\phi_A(f_i) = \frac{a_i^2 + b_i^2}{2\,\Delta f}$$

where $\Delta f = 1/T$. If we integrate from 0 to infinity, then

$$\int_0^\infty \phi(f_i)\,df_i = (A - \overline{A})^2$$

which is the variance of A. The autospectrum for a single frequency is a single number which is the contribution at that frequency to the total variance. One can see how these relations arise by squaring the original Fourier series and averaging, which yields

$$(A - \overline{A})^2 = \Sigma \frac{a_i^2 + b_i^2}{2}$$

because only sine^2 and cosine^2 have non-zero averages.

The cross-spectrum is the comparison of the spectra between two variables, usually to determine how much they are related. Let us first discuss the cospectrum and define a second Fourier series for B, similar to that for A, except a_i and b_i are replaced by c_i and d_i. The cospectrum is constructed by multiplying the two Fourier series together and averaging so that

$$CO_{AB}(f_i) = \frac{a_i c_i + b_i d_i}{2\,\Delta f} \quad .$$

The integral of the cospectrum over all frequencies is

$$\int_0^\infty CO_{AB}(f_i)\,df_i = (A - \overline{A})(B - \overline{B})$$

which is the covariance of A and B. Thus, the cospectrum of a single frequency is the contribution of the in-phase components to the total

cross-spectrum of A and B. The other part of the cross-spectrum is the quadrature spectrum. The quadrature spectrum is constructed by shifting the phase at each frequency by 90^{o} in the B series and multiplying the two series together and averaging. The result is

$$QD_{AB}(f_i) = \frac{a_i d_i - c_i b_i}{2\Delta f} \quad ;$$

the quadrature spectrum is a measure of the contribution of the 90^{o} out-of-phase components for each frequency to the cross-spectrum.

The cross-spectrum may be thought of in terms of a complex vector, as

$$S_{AB}(f_i) = CO_{AB}(f_i) + jQD_{AB}(f_i) \quad .$$

We can define a phase angle as,

$$\text{Phase } (f_i) = \text{Arc Tan } [\frac{QD_{AB}(f_i)}{CO_{AB}(f_i)}] \quad .$$

Thus, the phase is analogous to the angle between two vectors.

For the in-phase components of our two variables, the correlation is significant. The correlation varies between +1 and -1, and is an indication of how well the two variables are related, provided that they are in phase. The correlation between A and B is given by:

$$COR(f_i) = \frac{CO(f_i)}{\sqrt{\phi_A(f_i) \cdot \phi_B(f_i)}} \quad .$$

The coherence squared is a measure of the relationship like the correlation. The difference between the correlation and coherence

squared is that the latter measures how well A and B are related regardless of the phase. The coherence squared between A and B is given by:

$$COHSQD(f_i) = \frac{CO(f_i)^2 + QD(f_i)^2}{\phi_A(f_i) \cdot \phi_B(f_i)} \quad .$$

The coherence squared ranges from 0 for unrelated quantities to 1 for perfectly related quantities. It measures the fraction of the variance in one signal that is related to the other. Coherence (or $\sqrt{\text{coherence squared}}$) measures the fraction of amplitude that is related.

In addition to the cross-spectrum, another method of time series analysis is transfer functions. The basic principal of transfer functions is that from the spectrum of a "causing" or "forcing" variable, we can calculate the result in the "effected" variable. The transfer function between A and B is calculated by:

$$TR(f_i) = \sqrt{COHSQD(f_i) \cdot \frac{\phi_B(f_i)}{\phi_A(f_i)}} \quad .$$

If the two variables are thought to be closely related and the coherence squared is close to 1.0, we may calculate the transfer by

$$TR(f_i) = \sqrt{\frac{\phi_B(f_i)}{\phi_A(f_i)}} \quad .$$

The transfer function may be thought of as a predictor. Given the input amplitude at a certain frequency, we can predict the resulting output amplitude for that frequency.

We can smooth our spectral results by band averaging the cross spectra. Band averaging consists of taking the simple numerical average of groups or bands of frequency amplitudes. As an example, the band average of the first k frequencies of the autospectrum of A is

$$\phi(f_L) = \frac{1}{k} \sum_{i=1}^{k} \phi(f_i) = \frac{1}{k} \sum_{i=1}^{k} \left(\frac{a_i^2 + b_i^2}{2\Delta f}\right)$$

where $L = (k+1)/2$. Band averaging smooths the spectrum and results in more statistically reliable estimates.

Calculations

The motion of the buoy was computed for the center of gyration of the buoy. The center of gyration should be close to the center of drag due to the shape of the buoy. The toroids under the water line may be approximated as a cylinder; so the center of flotation will be at the symmetrical center of the approximated cylinder. In Appendix II, it is demonstrated that the center of gyration is approximately the center of flotation. The approximated cylinder of the toroids also presents most of the area that the wave forces will be acting on, as the lower part of the buoy is tower tubing and offers small cross sections by comparison. The result is that the approximate center of

the subsurface toroids will also be the center of drag, center of flotation, and center of gyration.

Almost all variables had to be corrected for the motion of the buoy. Once corrected, the variables were Fast Fourier transformed and analyzed spectrally. The two variables that were not affected by buoy motion were the tilts. The gyroscope measured the tilting of the buoy from stationary earth coordinates. Thus, no correction of the tilts was necessary. The x coordinate is chosen positive, outward from the face of the tower on which the wave poles are mounted (and thus points approximately opposite to the direction in which the waves are traveling). The z axis is positive upwards and the positive y axis is chosen to give a right-handed system. θX and θY, the tilts in the xz and yz planes, respectively, are taken to be positive when the top of the tower has a positive displacement relative to the center of gyration.

Unlike the tilts, the measured horizontal accelerations a1 (x direction) and a2 (y direction) had to be corrected for gravity and angular acceleration. It was assumed that the tower did little spinning or horizontal rotating. This assumption is based on the fact that the buoy was tethered to the ship by a sea cable and bridle which restricted horizontal rotation. In addition, the radius of gyration about the horizontal axis is very short--only a few centimeters--making the effect of the spin rotation negligible compared to the gravitational

acceleration. Therefore, we assumed that all of the angular motion of the buoy was due to tilting from the vertical.

A tilt off vertical introduces a false acceleration due to the earth's gravity. This value is $-g \sin \theta X$, where g is the acceleration of gravity--981 cm/sec^2. This false acceleration is subtracted from the measured acceleration. Likewise $-g \sin \theta Y$ must be subtracted from a_2.

Another required correction that needed to be made in the horizontal accelerations involved angular accelerations. The measured accelerations will include additional accelerations because the accelerometer is not at the center of gyration and drag. The calculation of the angular accelerations was done by spectral means. The angular acceleration was computed by Fast Fourier Transforming the θX and θY data and multiplying the Fourier coefficients for the first 64 frequencies by $-4\ \pi^2 f^2$, which is equivalent to double differentiation in the time domain. The 64th frequency, which corresponds to 0.51 Hz, has no information above it except noise. Therefore, the remaining higher frequencies were set to zero. Double differentiation accentuates the high frequencies and any noise at these frequencies. The procedure used here, which was chosen after preliminary examination of the θX, θY spectra, insures that reliable, low noise second derivatives are obtained. The $D^2\theta X/Dt^2$, $D^2\theta Y/Dt^2$ coefficients were inverse transformed back to time space. Now $R \cdot D^2\theta X/Dt^2$ is the

contribution of the angular acceleration to a1. R is the radius of gyration of the buoy, 4.5 m (see Appendix I for calculation). A similar procedure was used to find $R \cdot D^2\theta / Dt^2$, the angular acceleration in the y direction.

The two horizontal accelerations, A1 and A2, in buoy coordinates are given by:

$$A1 = a1 + g \sin \theta X - R \frac{d^2 \theta X}{dt^2}$$

$$A2 = a2 + g \sin \theta Y - R \frac{d^2 \theta Y}{dt^2} \quad .$$

The vertical acceleration also had to be corrected for gravity and for the centrifugal acceleration due to the angular velocity of the buoy off vertical, or $d\phi / dt$. The angle ϕ, the tilt from vertical, was calculated by using a small angle approximation, $\tan \phi = \phi$, since the angle is 10° or less. The result was:

$$\phi = (\theta X^2 + \theta Y^2)^{1/2} \quad .$$

The angular velocity, $d\phi / dt$ was calculated by a six difference finite differentiation, or:

$$\frac{\Delta \phi (I)}{\Delta t} = \frac{8 \cdot \phi (I+1) - 8 \cdot \phi (I-1) - \phi (I+2) + (I-2)}{\Delta t} \quad .$$

It was found that this finite differentiation approximated the derivative to within 1 or 2%. The total centrifugal acceleration is given by:

$$R \left(\frac{d\phi}{dt}\right)^2 \quad .$$

The centrifugal acceleration correction was a small correction to the vertical acceleration, of order 5-10%. Ignoring this correction or correcting to the center of mass instead of the center of drag and gyration would make very little difference to the final results.

The important correction to the vertical acceleration was for the earth's gravity. A tilt of the tower off vertical resulted in the accelerometer indicating a false acceleration $-g(1-\cos\phi)$. The vertical acceleration, A3, corrected to tower coordinates is:

$$A3 = a3 + g(1-\cos\phi) - R\left(\frac{d\phi}{dt}\right)^2$$

where a3 is the measured vertical acceleration.

Once all of the three accelerations were corrected to the tower coordinate system, it was necessary to rotate them to a stationary vertical coordinate system. If the stationary horizontal accelerations are AX and AY, and the vertical acceleration is AZ, then the final stationary accelerations are

$$AX = A1 \cdot \cos\theta X + A3 \cdot \sin\theta X$$

$$AY = A2 \cdot \cos\theta Y + A3 \cdot \sin\theta Y$$

$$AZ = -A1 \cdot \sin\theta X + A2 \cdot \sin\theta Y + A3 \cdot \cos\phi \ .$$

These rotation corrections are small--differences between A1 and AX, etc. are of order 10%.

Like the accelerations, the sea slopes were corrected for the buoy motion. As we saw from Figure 2, the sea slope axes were

aligned at 45° to the motion instruments' coordinate system, and must first be rotated through 45° to align them with those of the motion instrument system. A wave slope is measured by the difference in resistance between two wave poles, which is calibrated to mean a certain distance. The slope is equal to the pole difference divided by the distance between poles. For both slopes, higher water in the negative x and y directions was defined as positive since then a + slope corresponds to a situation which one would expect to produce a + tilt. Since the measured rotated slopes, s1 and s2 are aligned with the tilt axes θX and θY, positive tilts of the buoy add false slope angles of $-\theta X$ and $-\theta Y$, respectively. This false slope must be subtracted from the measured sea slopes, s1 and s2, to get the actual sea slopes, SX and SY, which are given by:

$$SX = s1 + \theta X$$

$$SY = s2 + \theta Y \ .$$

The wave height was measured by the center wave pole used to obtain the slopes. The wave height pole was on an arm aligned with the motion systems instrument x axis. Higher water at the pole was considered more positive. A positive θX tilt of the buoy introduces an apparent positive wave height,

$$D \tan (\theta X),$$

where D is the distance from the center of the tower (79 cm), which must be subtracted from the measured wave height to get the true wave

height. Since θX is typically less than 5^{o}, we may use the small angle assumption; that is,

$$\tan \theta X \approx \theta X \ .$$

The wave height relative to the buoy, η, is then given by:

$$\eta = W - D \cdot \theta X,$$

where W = measured wave height.

To obtain the wave height relative to a stationary coordinate system one must correct for the vertical displacement of the buoy. To find the displacement of the buoy, the vertical acceleration (corrected to stationary coordinates) was Fast Fourier Transformed and integrated twice by dividing the Fourier coefficients by $-(2\pi f_i)^2$. This procedure gives the vertical displacement of the buoy in frequency space, which was added to the Fast Fourier Transformed corrected wave height. The final result was a Fourier series representing the actual wave height in a stationary coordinate system.

Spectral Averages

A record was divided into blocks of 1,024 points. Thus 512 spectral estimates are obtained, one for each fundamental frequency band, with frequencies from 0.008 Hz to 4.17 Hz. The spectra for each block were band averaged for each variable according to two methods. The first was a logarithmic scheme which took the four

lowest frequencies individually, then produced two averages of two fundamental frequency bands, two of four frequency bands, two of eight frequency bands; up to two of 128 frequency bands. The result was a power spectrum band averaged into 18 bands. This logarithmic form of band averaging gives approximately equal spacing of points on a logf plot which allows one to plot a wide frequency range on a single plot. $f\phi$ versus logf is used on such a plot since such a plot conserves variance, that is,

$$\int f\phi \, d\ln f = \int \phi \, df$$

Logf is used rather than lnf since frequencies are more identifiable from log f than lnf. The area under an $f\phi$ log f plot is proportional to the variance.

The second averaging scheme was a simple average over two fundamental frequency bands. This scheme started with the 9th frequency (0.077 Hz) and went to the 20th frequency (0.257 Hz). This two-band average scheme gave more detail in the wave band, where most of the important energy is.

The results of all blocks were averaged over a given record. These included 30 band averages for each of the variables, and co- and quad-spectra for each of the five pairs of crosspectra (θX, SX; θX, SX; AX, SX; AY, SY; AZ, η). The integrals of co- and quad-spectra and autospectra were also averaged over the whole record. The resultant record band averages of co- and quad-spectra were used to

calculate the phase, coherence and transfer functions for each of the five cross-spectra for the whole record.

IV. RESULTS

Autospectra

Table 1 gives the root mean square values, σ, for the eight variables. Table 2 gives the peak spectral values for the eight variables. Record 1 is about 30 minutes long; Records 2 and 3 are each 15 minutes long.

There is little energy in the variables except in the wave band, so graphs of the autospectra will only be shown in the vicinity of the wave band. The plots will be $f\phi$ log f. Each point up to 0.257 Hz is an average of two fundamental frequency bands averaged over the whole record.

The degrees of freedom in the two frequency band averages are equal to 4 N, where N = number of blocks. Thus Record 1 has 56 degrees of freedom for the two band averages, and the Records 2 and 3 each have 28 degrees of freedom. The equivalent degrees of freedom can be computed from the variance of the spectral estimates from block to block, and they approximately agree with the above estimates. Hence, in this respect, the signals obey Gaussian statistics.

Above f = 0.257 Hz, the points represent logarithmic band averages; each band again averaged over all blocks in the record. Since even more frequencies go into making up these higher bands,

Table 1. RMS values.

Variable/Record		1	2	3
σ_{SX}	Radians	.0761	.0971	.0945
	Degrees	4.36	5.56	5.42
σ_{SY}	Radians	.0640	.1160	.0776
	Degrees	3.67	6.64	4.45
σ_{η} (disregarding 6 lowest frequencies)	cm	33.9	49.7	45.6
$\sigma_{\theta X}$	Radians	.0448	.0613	.0624
	Degrees	2.57	3.51	3.58
$\sigma_{\theta X}$	Radians	.0394	.0428	.0426
	Degrees	2.26	2.45	2.44
σ_{AX}	cm/sec^2	28.7	65.4	64.4
σ_{AY}	cm/sec^2	24.7	30.9	29.7
σ_{AZ}	cm/sec^2	28.0	52.0	46.3

Table 2. Peak spectral values.

Variable/Record		1	2	3
Φ_{SX}	rad^2 sec	.1060	.0670	.1160
Φ_{SY}	rad^2 sec	.0216	.1100	.1030
Φ_{η}	cm^2 sec (wave band)	14,500	28,500	28,600
$\Phi_{\theta X}$	rad^2 sec	.0462	.0552	.0762
$\Phi_{\theta Y}$	rad^2 sec	.0276	.0251	.0351
Φ_{AX}	cm^2/sec	10,600	40,300	62,700
Φ_{AY}	cm^2/sec	6,060	4,870	5,770
Φ_{AZ}	cm^2/sec	4,670	27,700	17,900

their degrees of freedom are even larger.

The sea response is represented by the spectra of two wave slopes and the wave height. The spectral forms of the two wave slopes, SX and SY, are very similar as may be seen in Figure 7. In both cases, there is very little energy at frequencies less than 0.1 Hz or greater than 1 Hz. The wave slope energy is largely associated with the frequencies from 0.1 to about 0.3 Hz, with a peak around 0.12 Hz. In the slopes, there appears to be more energy in the x direction than in the y in Record 1.

The wave height autospectrum is less well-defined than the slope autospectrum. The low frequency end of the spectrum is distorted. The values go up rapidly at frequencies lower than those shown in Figure 8 and the values for the three lowest frequencies on the figure are probably too large. The energy associated with wave heights at frequencies greater than 1 Hz is negligible. The maximum energy in the wave band is associated with frequencies between 0.12 and 0.3 Hz.

Anomalously large values for low frequencies are experienced with the wave height. The wave height is obtained by integrating the vertical acceleration twice in frequency space. The vertical acceleration is corrected for gravity and rotated to stationary coordinates before integration. Examination of the numerically twice-integrated vertical acceleration showed that it is insensitive to rotation and the

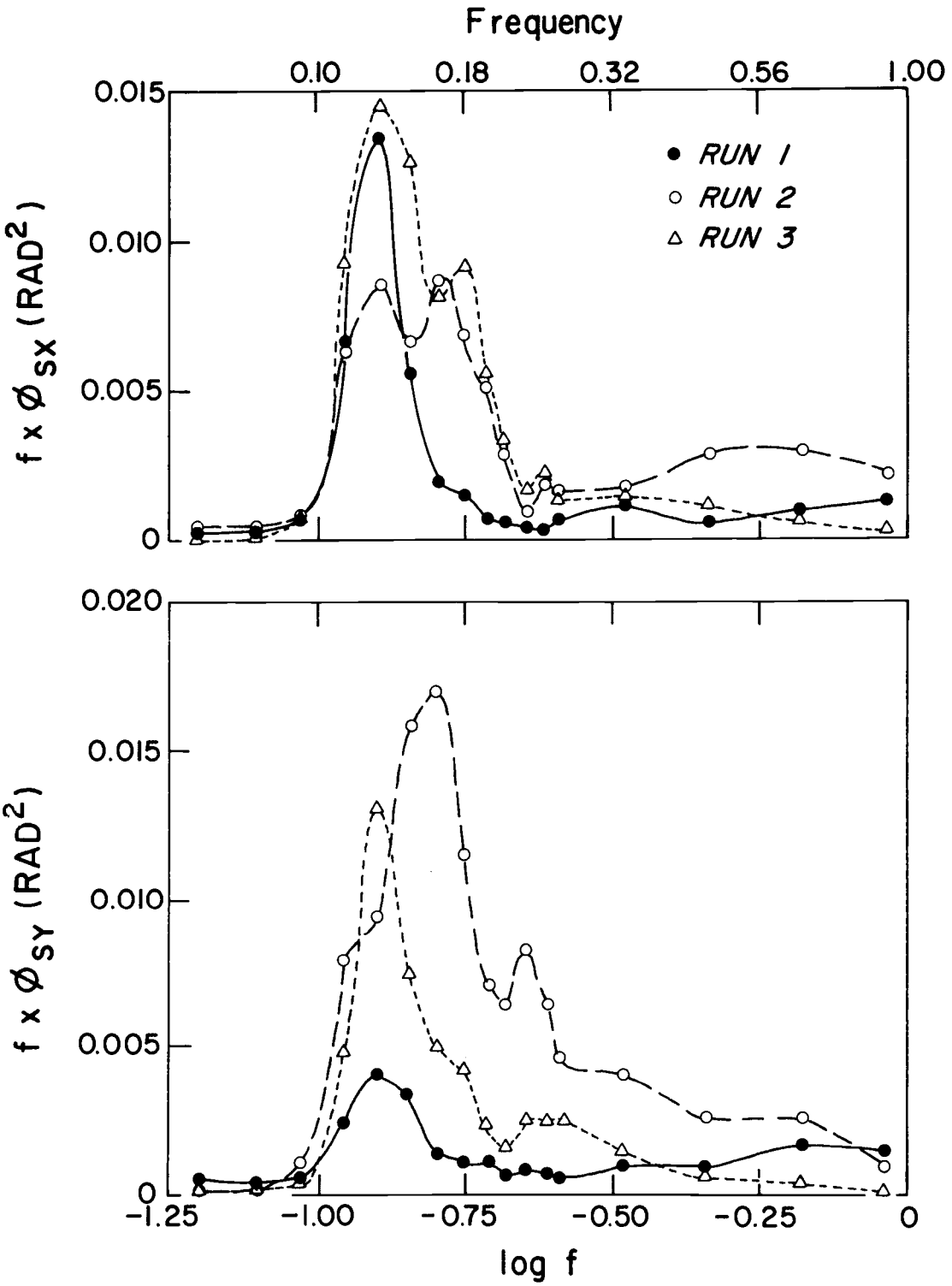

Figure 7. Autospectrums of wave slopes, SX and SY.

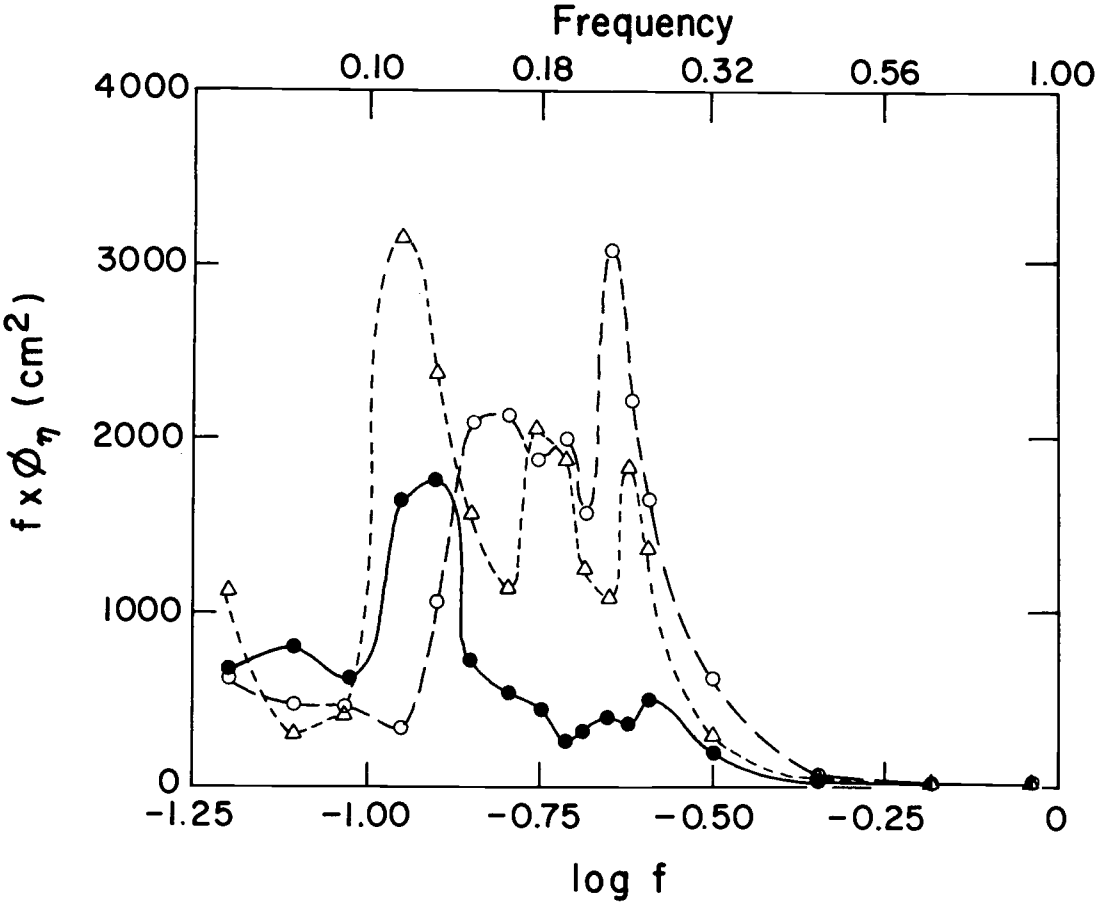

Figure 8. Autospectrum of wave height, η.

variation of the radius of gyration. However, the correction of the accelerometer for the acceleration of gravity is significant. There is a large variation of about 0.016 Hz (1 cycle per minute) in the twice-integrated acceleration. This low frequency variation is probably caused by precession of the gyroscope which is not totally compensated for by the instrument. The precessional effects would be largest when the wave amplitudes were largest. The separation between large amplitudes (groups) is about 1 minute.

Since the tilt of the buoy, measured by the gyroscope, is used to correct for the variations of the vertical acceleration, there is a spurious 1 cpm signal in the twice-integrated vertical acceleration. Attempts to remove the spurious signal by linear detrending before integration prove only partially successful. The result was that the lowest 4 to 6 values of the wave height spectrum are not correct but a result of instrumentation. The problem could be corrected by using a gyroscope with a better precessional correction. Despite the difficulties with the lowest 4 to 6 frequencies, it is felt that the wave band (0.1-0.3 Hz) of the wave height autospectrum is reliable as far as general shape and values, although the spectral values may be a bit large near 0.1 Hz. Extension of the downward trend of the low frequency values suggests that the errors are not too large. In calculating the total variance to get RMS values for η the contributions at frequencies below 0.077 Hz ($\log f = -1.11$) are omitted.

From the autospectra of the slopes and wave heights, we have a definition of the functions driving the buoy. Since the mean square slope energy is greater in the x direction than the y for Records 1 and 3, we know that more wave energy is coming in the x direction for these records. In Record 2 the RMS slopes are about equal for the two directions. There is more wave energy in the wave slopes and wave height in Records 2 and 3 than Record 1. Record 1, the longest in real time, tends to be more smooth in its wave slope and wave height spectra.

The buoy's response to the sea is represented by the spectra of the two tilts and three accelerations. The spectra of the two tilts of the buoy, θX and θY, are similar except for θX being greater than θY. The tilt spectra are similar to the wave slope spectra except that the tilts had a much more rapid cut-off of energy above about 0.26 Hz, as one might expect since the buoy should filter out higher frequencies. There is a narrow band associated with the tilts from 0.118 to 0.167 Hz, which contains most of the energy associated with the tilts (see Figure 9). In RMS values θX and θY are about 0.6 times SX and SY respectively.

The horizontal accelerations spectra of the buoy are broader than the tilts spectra (see Figure 10). Accelerations are second derivatives of displacements and so their spectra will have accented higher frequencies and suppressed lower frequencies compared to

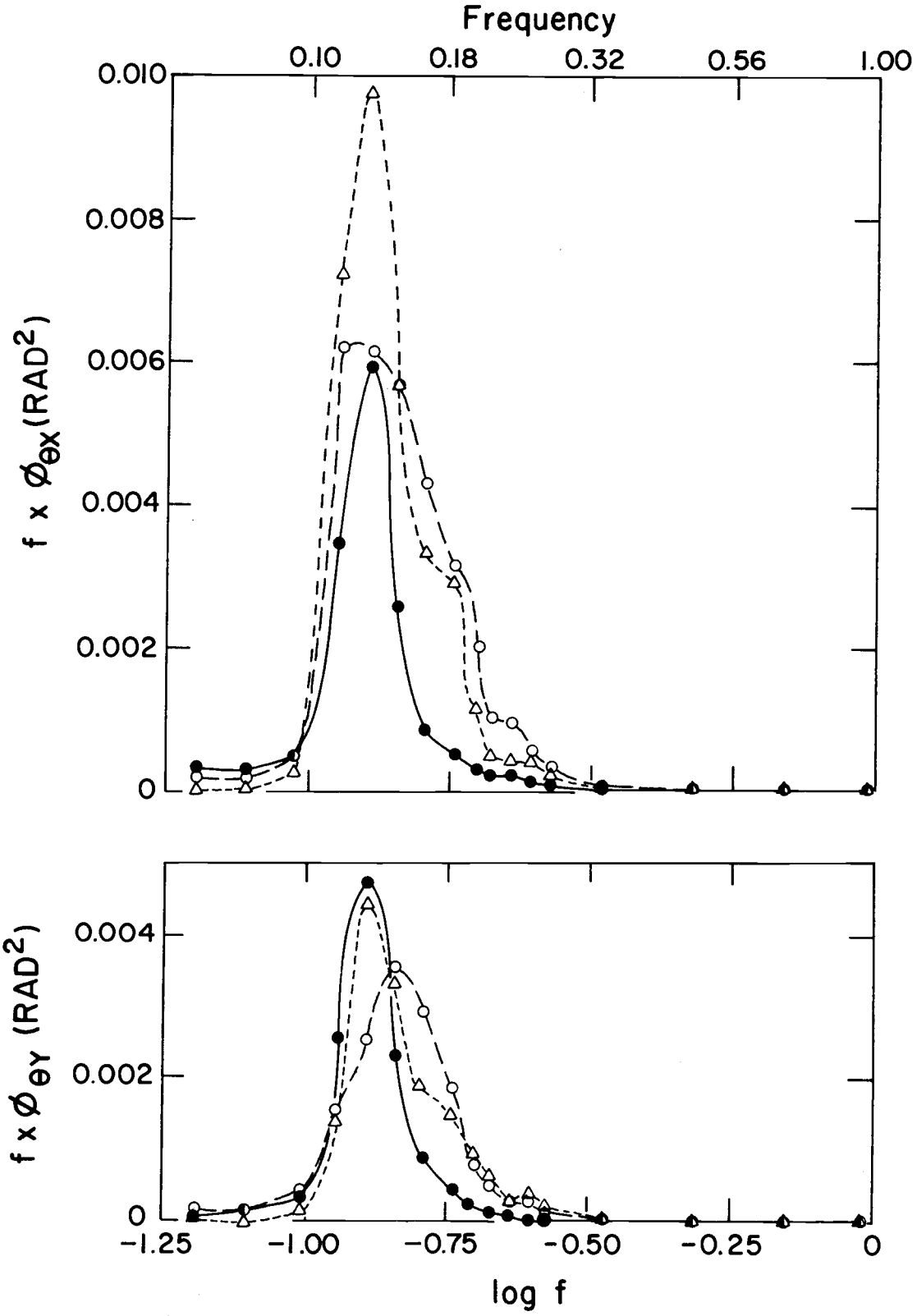

Figure 9. Autospectrums of buoy tilts, θX and θY.

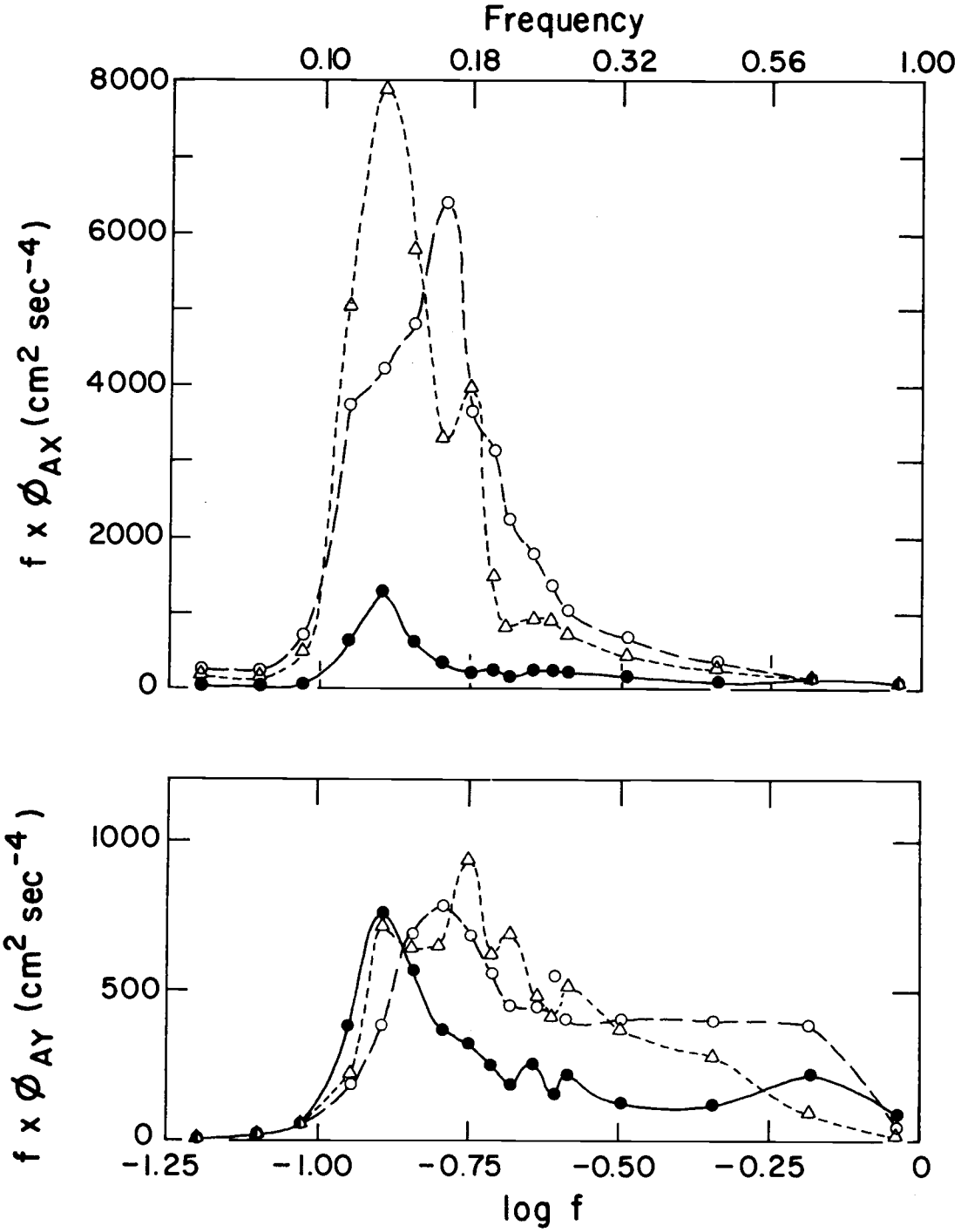

Figure 10. Autospectrums of buoy accelerations, AX and AY.

displacement spectra from which they are derived. There is a sharp increase in energy at 0.1 Hz with peaks between 0.118 and 0.167 Hz, and negligible energy at frequencies greater than 1.0 Hz. Of the three records, Record 1 has significantly smaller amplitudes; a reflection of the smaller driving energy in the waves for Record 1. The x acceleration always has significantly more energy than the y acceleration (note the difference in scales in Figure 10) as one might expect since the predominate wave direction tends to be in the x direction and extra accelerations due to ship pulling on the buoy would be mainly in the x direction.

There is some difficulty with the x acceleration signals. The x acceleration signal in Record 2 appears to be somewhat choppy, but even more so in Record 3. It is thought that the accelerometer was sticking somewhat on the x axis and so not recording the x acceleration properly.

AZ has the same general spectral shape as the horizontal accelerations (see Figure 11). Record 1 has much less energy than the other two records. There is a sharp increase in energy at 0.1 Hz and little energy beyond about 0.4 Hz. The peak energy is at slightly higher frequencies than the wave heights and slopes.

Now that we have looked at the tilts and acceleration, we have a definition of the spectral form of the response of the buoy. The spectral energy is quite similar to the wave spectrum in peaks and

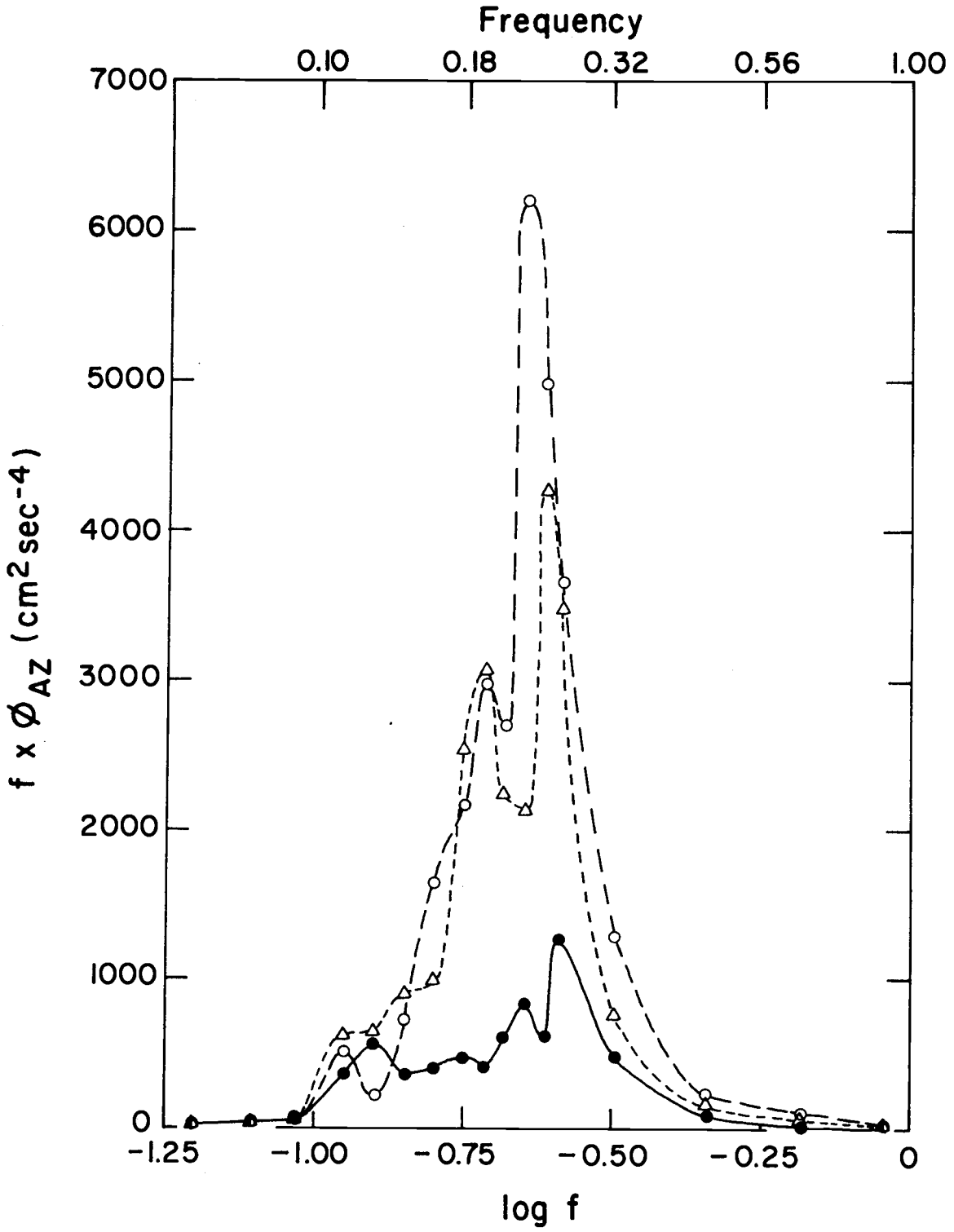

Figure 11. Autospectrum of the buoy vertical acceleration, AZ.

energy concentration in the wave band. The larger energy of θX and AX reflects the fact that the predominate wave energy is in the x direction. Of the three records, there is always more energy in the 2 and 3 records than the 1 record. The same is true of the wave slopes and wave heights. The longer 3 record is more regular and smooth than the other two, as was also reflected in the wave slopes and heights. The broader spectra for Records 2 and 3 suggest that there is mainly swell in Record 1, but sea and swell in Records 2 and 3.

Cross-spectra, Coherence and Phase

Now let us consider cross-spectra among variables. First let us discuss what one might expect. The cross-spectra were examined between the horizontal acceleration and the wave slope. Small amplitude wave theory gives the wave height as

$$\eta = a \sin (kx - \omega t)$$

The slope of the surface is given by

$$SX = \frac{\partial \eta}{\partial x} = ak \cos (kx - \omega t)$$

The horizontal velocity is given by

$$V = \frac{agk}{\omega} \cdot \frac{\cosh k (h + z)}{\cosh kh} \sin (kx - \omega t)$$

The horizontal acceleration is given by

$$AX = \frac{\partial U}{\partial t} = agk \frac{\cosh k (h + z)}{\cosh kh} \cos (kx - \omega t)$$

At the surface, $z = 0$, so

$$AX = agk \cos (kx - \omega t)$$

substituting in from SX,

$$AX = g\, SX \quad .$$

A similar relationship applies for the y direction. As a result, the slope of the sea surface is related to the water particle velocity acceleration in the same horizontal direction, and they are in phase.

The next cross-spectrum relationship reviewed is that between the vertical acceleration and the wave height. Again, for small amplitude wave theory, the vertical velocity is given by

$$W = \frac{\partial \eta}{\partial t}$$

and the vertical acceleration of the surface is

$$AZ = \frac{\partial^2 \eta}{\partial t^2} = -\omega^2 \eta \quad .$$

Thus, the vertical acceleration of the water surface, and presumably the buoy, are related to the wave height but they will be 180° out-of-phase.

Finally, the cross-spectra are studied between the slopes and the tilts. It is assumed that the sea slope SX is related to the buoy tilt θX, and both are in phase. A similar relationship holds for the y direction.

Now that we have an idea of what one may expect, let us consider the cross-spectra of the five pairs of variables. The first cross-spectra are between θX and SX, the tilt of the buoy and the wave slope in the same direction. The cospectra, coherence and phase may be seen in Figures 12 and 13. The average integral of the cospectrum for the three records was four times that of the quadrature spectrum, which is to be expected since the phase is close to zero. The slope and tilt are nearly in phase but there is more scatter at the higher frequencies. Most of the cospectral energy is associated with the 0.118 and 0.167 Hz frequencies, with the maximum at the former. The coherence is very high at low frequencies and decays quickly at frequencies greater than 0.3 Hz. Note that the coherence is only meaningful where there are appreciable spectral values.

The cross-spectra between the θY and SY are very similar to those between θX and SX. The cospectra, coherence and phase may be seen in Figures 14 and 15. Again, most of the cross-spectral information is in the cospectra and at frequencies from 0.118 to 0.167 Hz. There was generally a high coherence at low frequencies with a quick change then to low coherence just past the wave band. SY and θY are nearly in phase up to the wave peak of 0.118 Hz and then the phase begins to wander.

From the SX, θX and SY, θY cross-spectra, we see that the tilt of the buoy is closely related to sea slopes. In fact, the buoy is a sea surface follower with respect to slopes at low frequencies up through

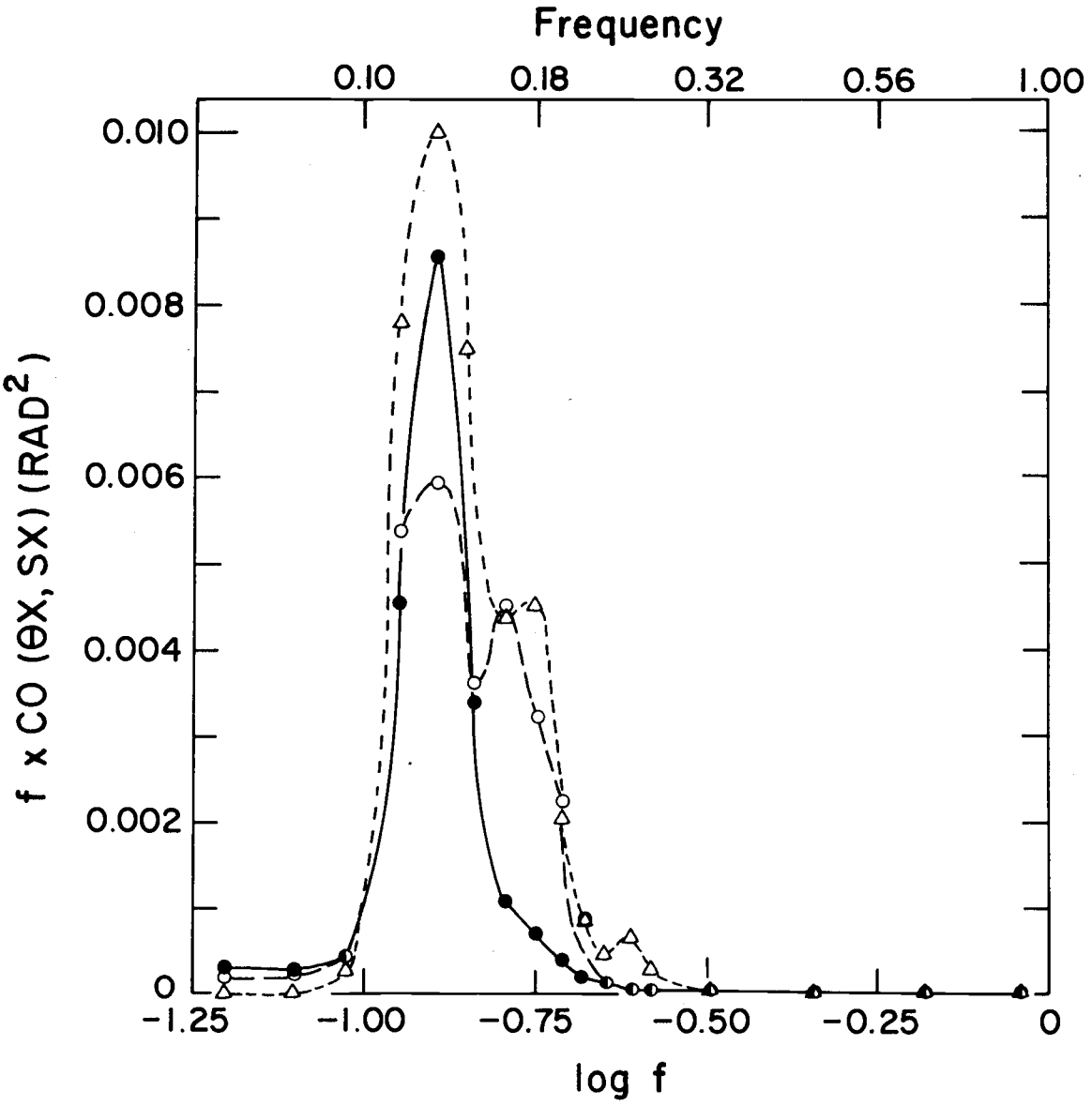

Figure 12. Cospectrum of buoy tilt, X, and wave slope, X (θX, SX).

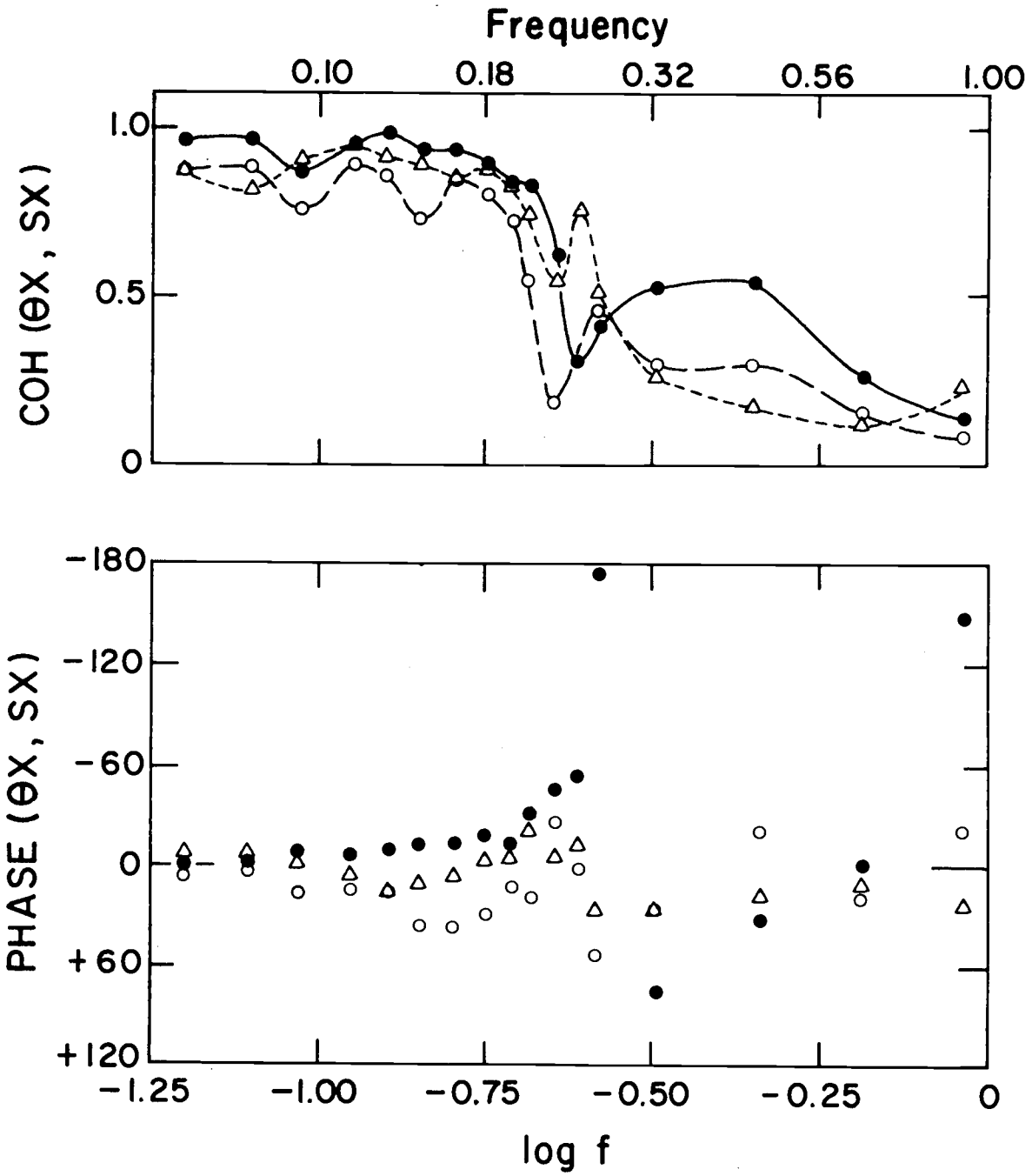

Figure 13. Coherence and phase of buoy tilt, X, and wave slope, X (θX, SX).

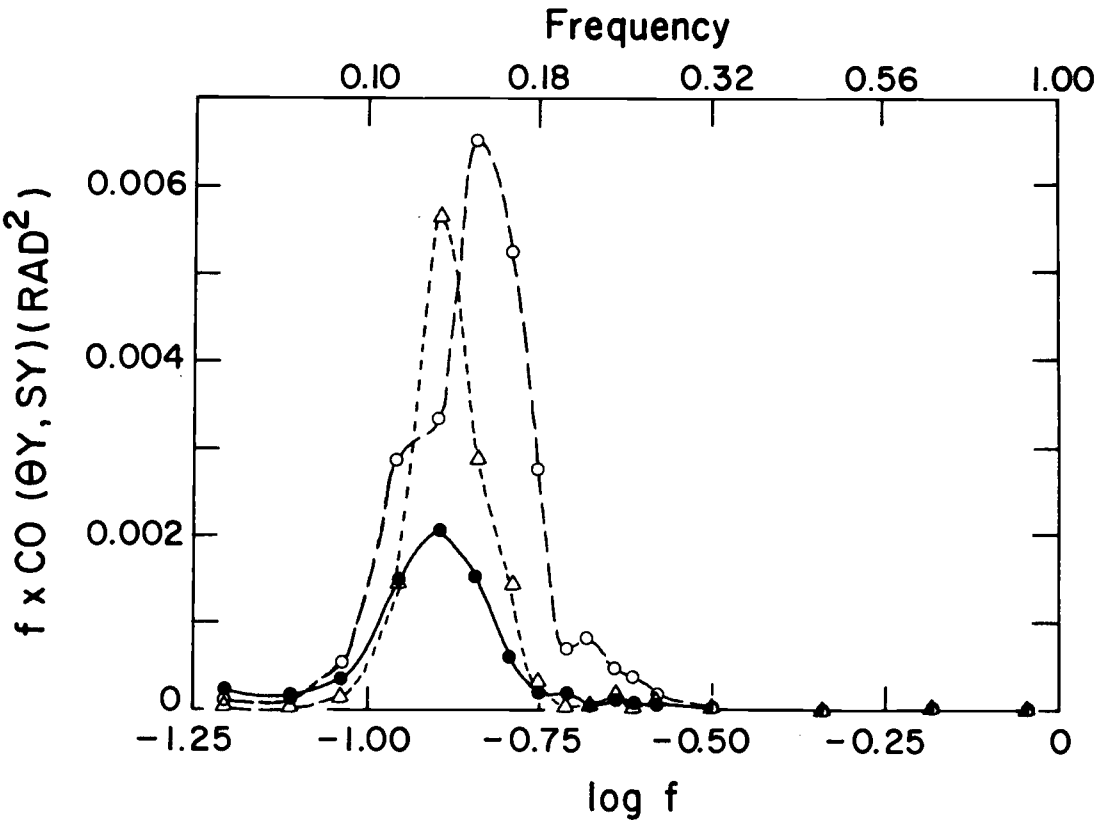

Figure 14. Cospectrum of buoy tilt, Y, and wave slope Y (θY, SY).

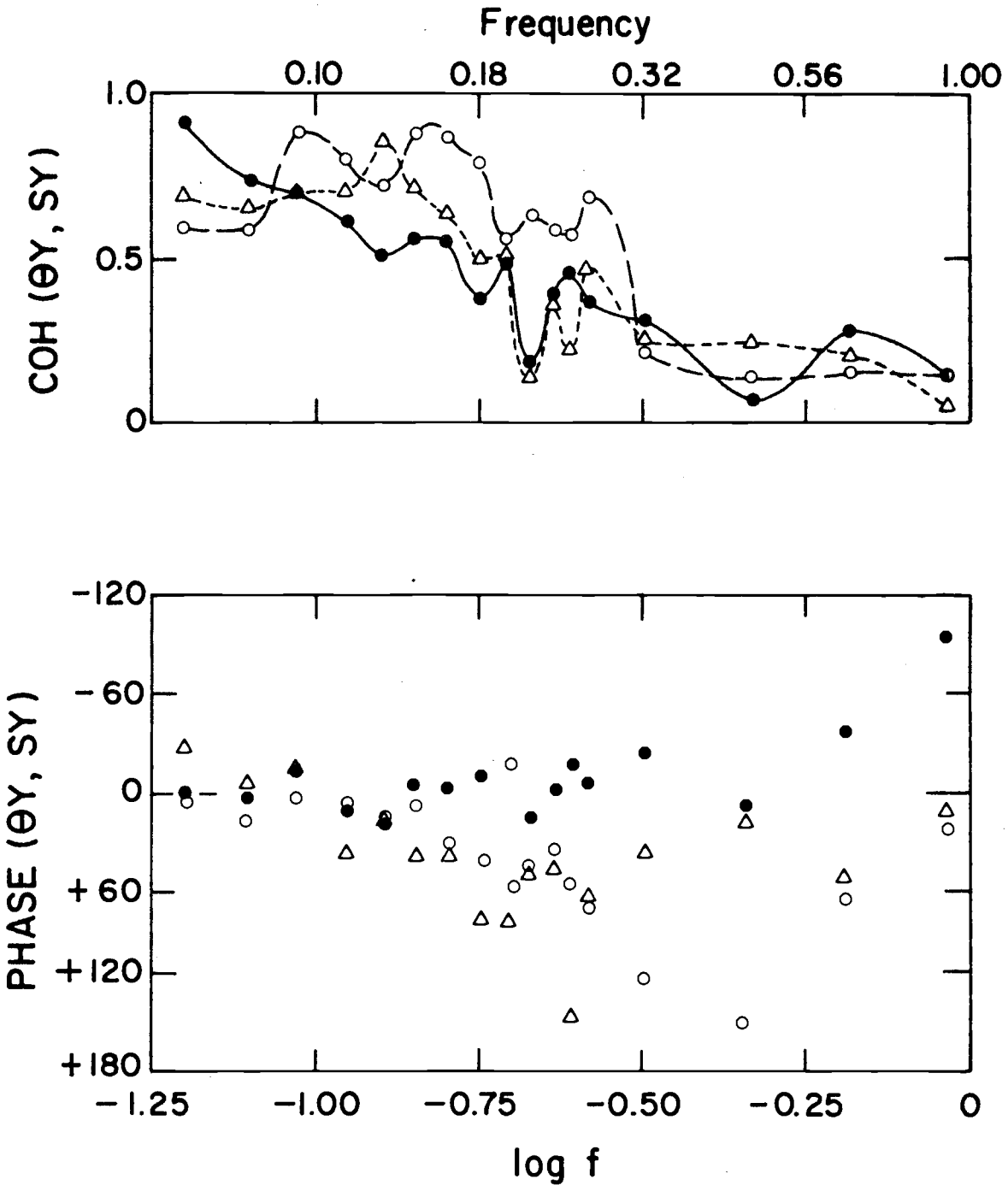

Figure 15. Coherence and phase of buoy tilt, Y, and wave slope, Y (θY, SY).

the wave band. Then, at frequencies above the wave band, the tilting of the buoy has little coherence with the sea surface slope. With respect to the tilts, therefore, the buoy is a swell follower, but tends to filter out the sea.

For AX-SX, there are comparable magnitudes in the co- and quadrature spectra, so both are plotted along with the coherence and phase (see Figures 16 and 17). Cospectra show that most of the contributions are between 0.1 and 0.3 Hz. The quadrature spectra show basically the same thing.

Record 1 is different from the other two in that the cospectrum is smaller than the quadrature spectrum. The coherence tends to be scattered, but it is high in the wave band.

The cross spectra between the AY and SY (Figures 18 and 19) show that they are not as well related as AX and SX. In general, the Record 1 has considerably lower cross-spectral values than the other two. The significant magnitudes of all three are spread between 0.1 and 0.7 Hz. The coherence of SY and AY shows a tendency for higher values in the wave band, and lower values at the higher and lower frequencies. The phase tends to wander but the trend is around 90°.

The cross spectra between AX-SX and AY-SY appear to be more complex than the tilt-slope relationships. The buoy's horizontal accelerations appear to be fairly coherent with sea surface and roughly 90° out-of-phase at the peak of the wave energy. However, at other

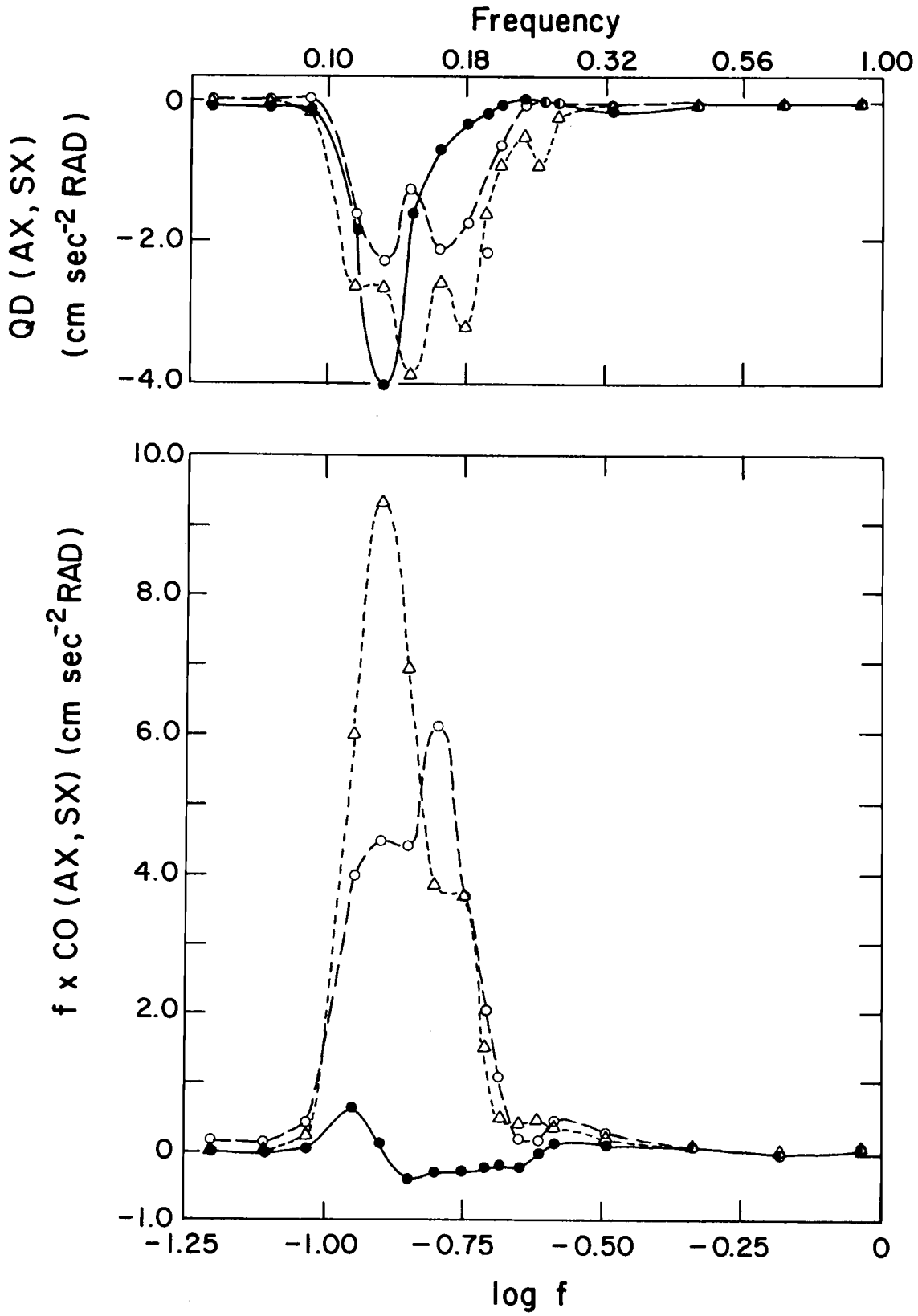

Figure 16. Cospectrum and quadrature spectrum of buoy acceleration, X, and wave slope, X (AX, SX).

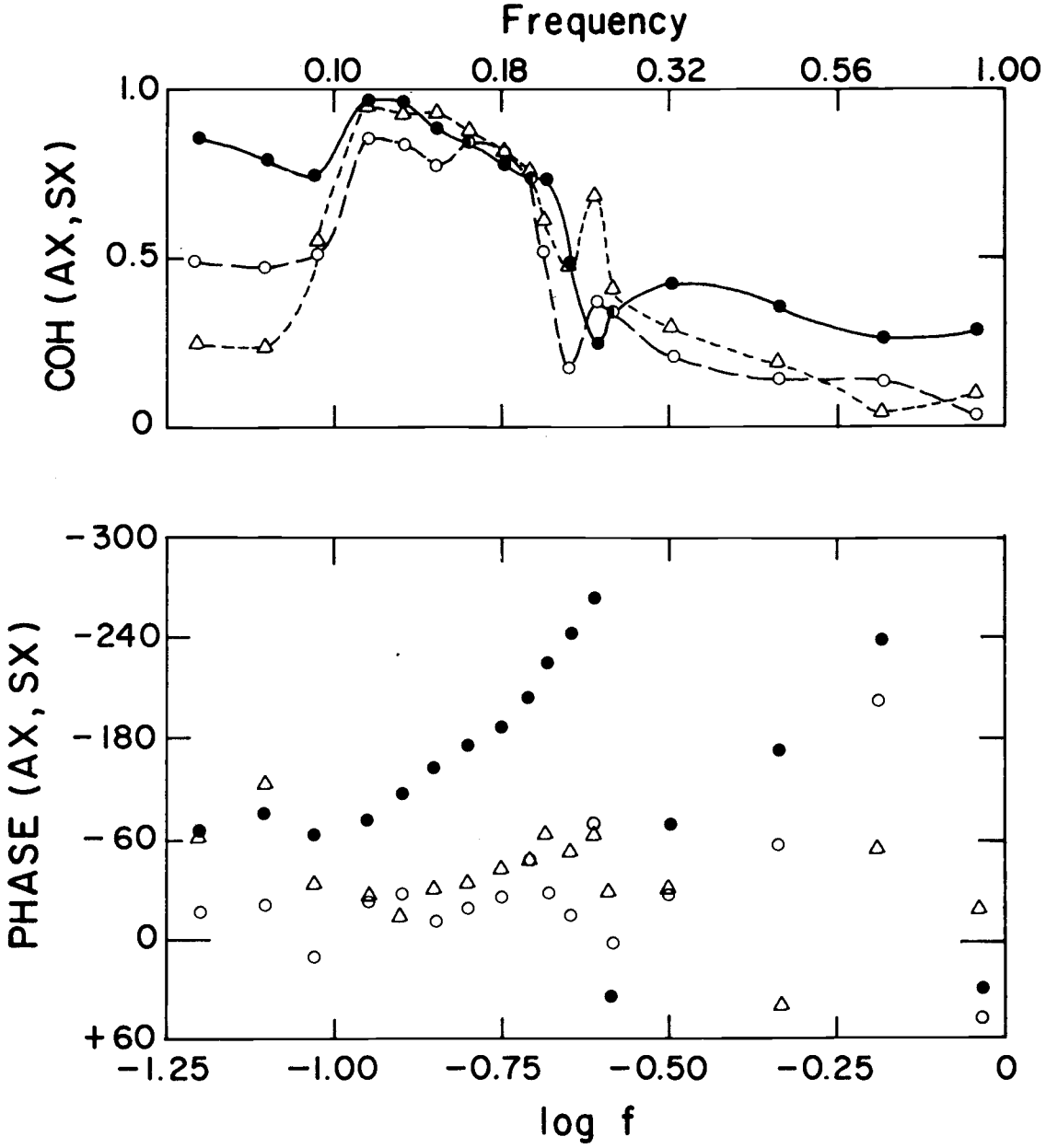

Figure 17. Coherence and phase of buoy tilt, X, and wave slope (AX, SX).

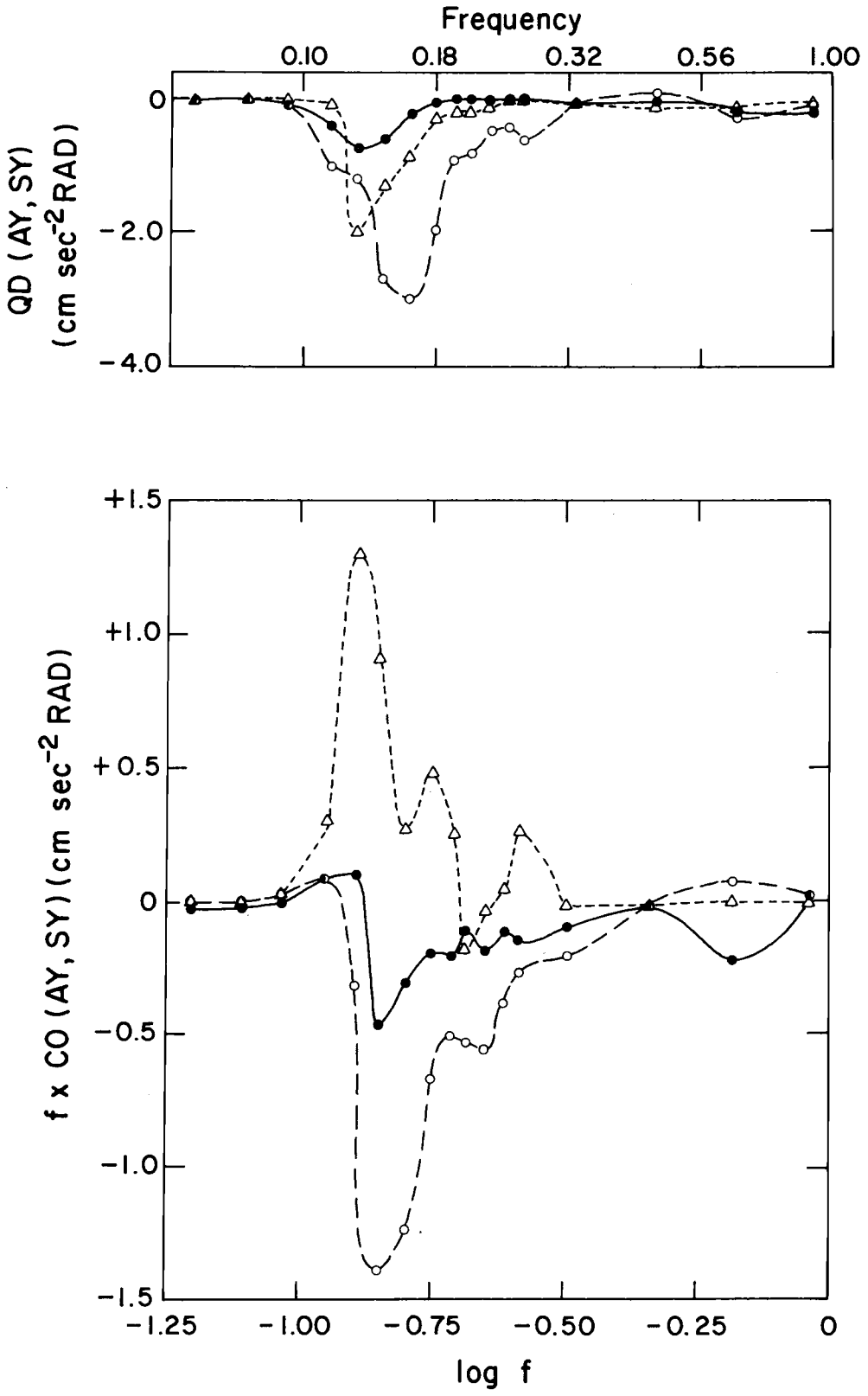

Figure 18. Cospectrum and quadrature spectrum of buoy acceleration, Y, and wave slope, Y.

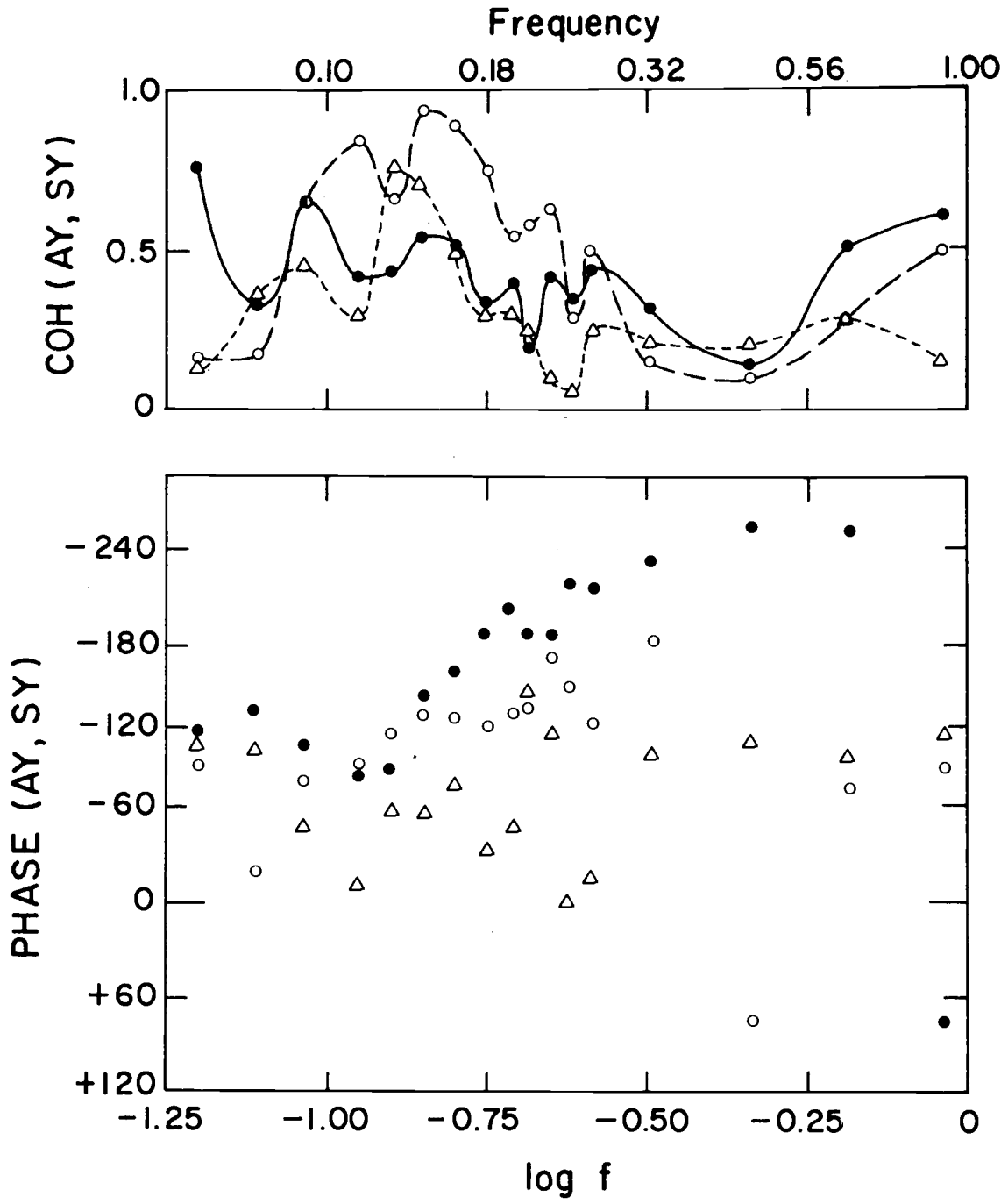

Figure 19. Coherence and phase of buoy acceleration, Y, and wave slope, Y (AY, SY).

than peak wave frequency, the picture is confused. At very low frequency, the buoy accelerations tend to be in phase with the slopes, and out-of-phase at high frequencies. There appears to be a rapid and large phase shift just after the wave peak frequency for all three records. Such behavior suggests that the natural frequency for tilts is near the center of the wave band.

The cross-spectra between the wave height and the vertical acceleration show a stronger relationship than that between the slopes and the horizontal accelerations. The cospectra are much larger than the quadrature spectra so the cospectra are plotted along with the coherence and phase in Figures 20 and 21. The cospectra are large only at frequencies between 0.1 and 0.7 Hz. The wave height and vertical acceleration have a coherence of almost +1 from the low frequencies to just past the wave band, or 0.6 Hz, and very quickly drop to negligible levels. The high coherence at lower frequencies is bound to occur since most of wave height comes from the double integration of the vertical acceleration of the buoy. The phase is almost 180^{o} until the frequency exceeds 0.5 Hz and then it begins to wander at the higher frequencies.

We have considered the five sets of cross-spectra and then coherence and phase. We note that perfect coherence does not occur between the buoy and the sea. This non-perfect coherence is due to the randomization of phase of the driving waves. In addition,

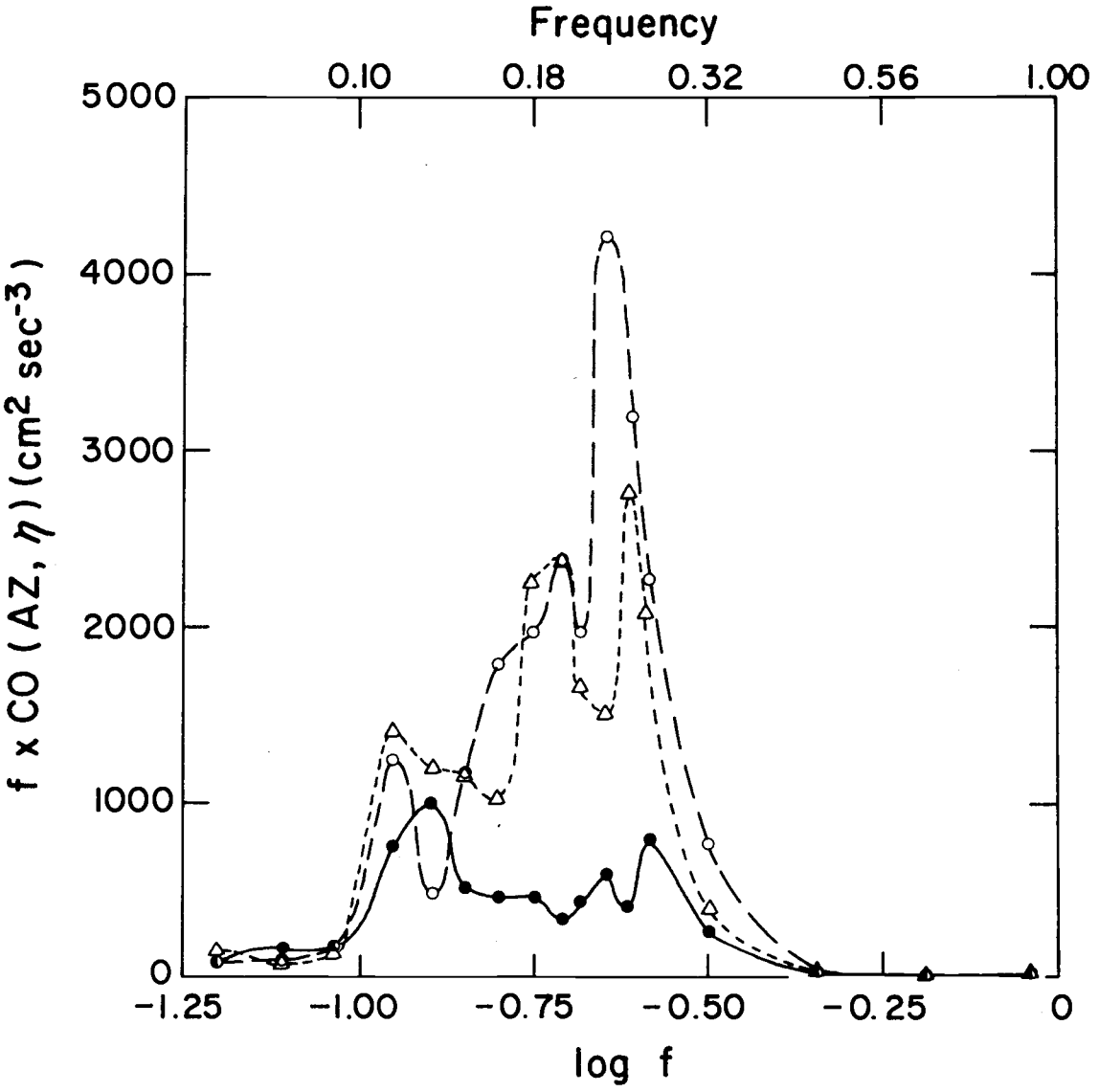

Figure 20. Cospectrum of buoy acceleration, Z, and wave height, η (Z, η).

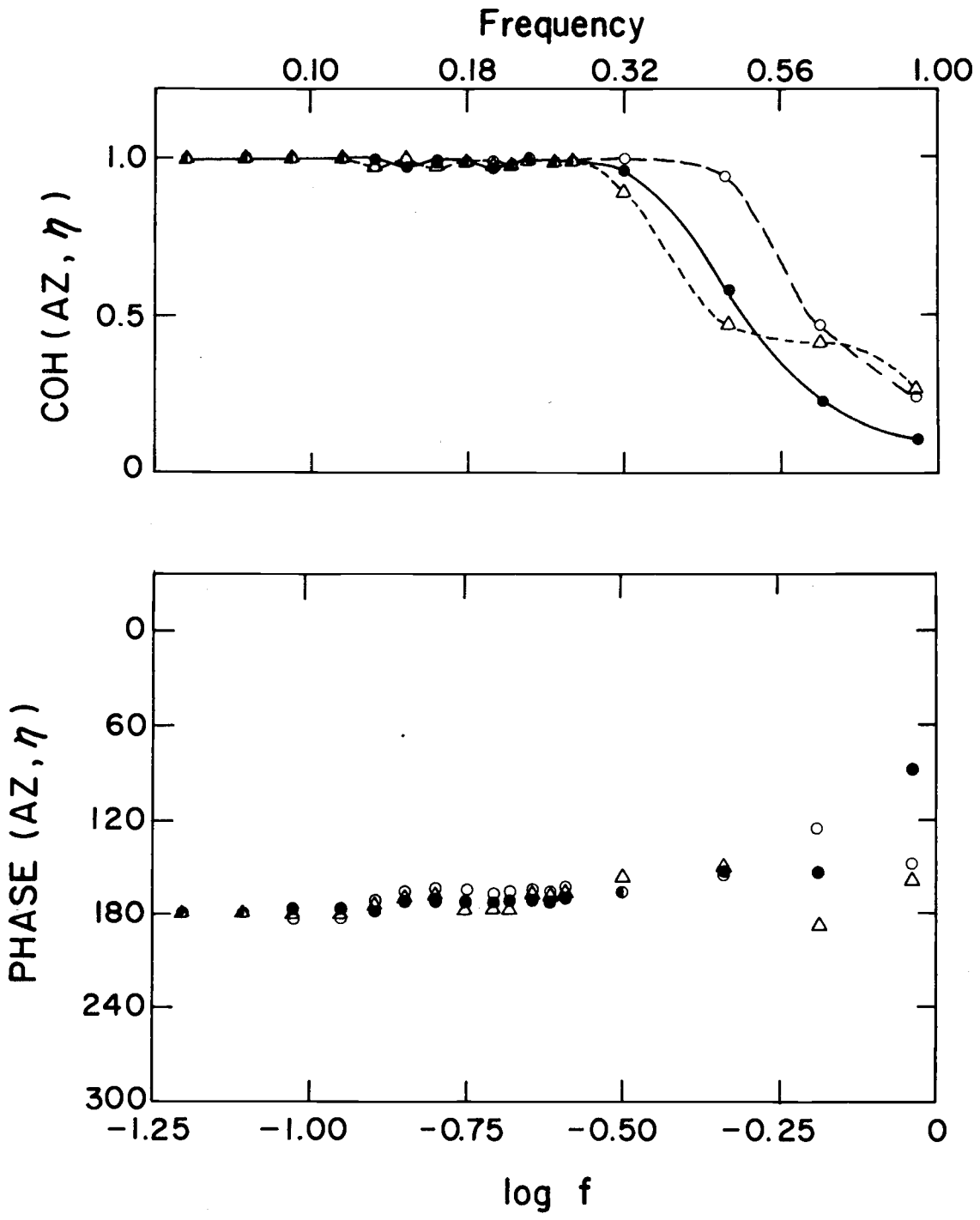

Figure 21. Coherence and phase of buoy acceleration, Z, and wave height, η (AZ, η).

there are ship effects, current and wind that are accelerating the buoy. However, the waves are clearly driving the buoy.

Transfer Functions

The last of the relationships that we shall consider among the five pairs of cross variables are the transfer functions. It is assumed that the waves are driving the buoy and the coherence is high. Therefore, the transfer function used will be

$$TR\ (B, A) = \sqrt{\frac{\phi_B(f_i)}{\phi_A(f_i)}}$$

where ϕ_A is the input spectrum and ϕ_B is the output spectrum. The phase relations which complete the transfer function description have already been shown. In order to get transfer functions such that 1.0 is the ideal relationship, some of the spectra are normalized according to the expected results discussed in the last sub-section. The input spectra ϕ_{SX}, ϕ_{SY} are multiplied by g^2 in calculating the transfer functions with AX, AY, respectively. Likewise ϕ_η is multiplied by ω^4 in calculating the transfer function with AZ.

The graphs of the transfer functions may be seen in Figures 22, 23, and 24. In the wave band, the transfer function of θX, SX is close to 0.8, while the θY, SY transfer function is more like 0.7. The buoy tends to tilt with the sea surface but damps the torques somewhat.

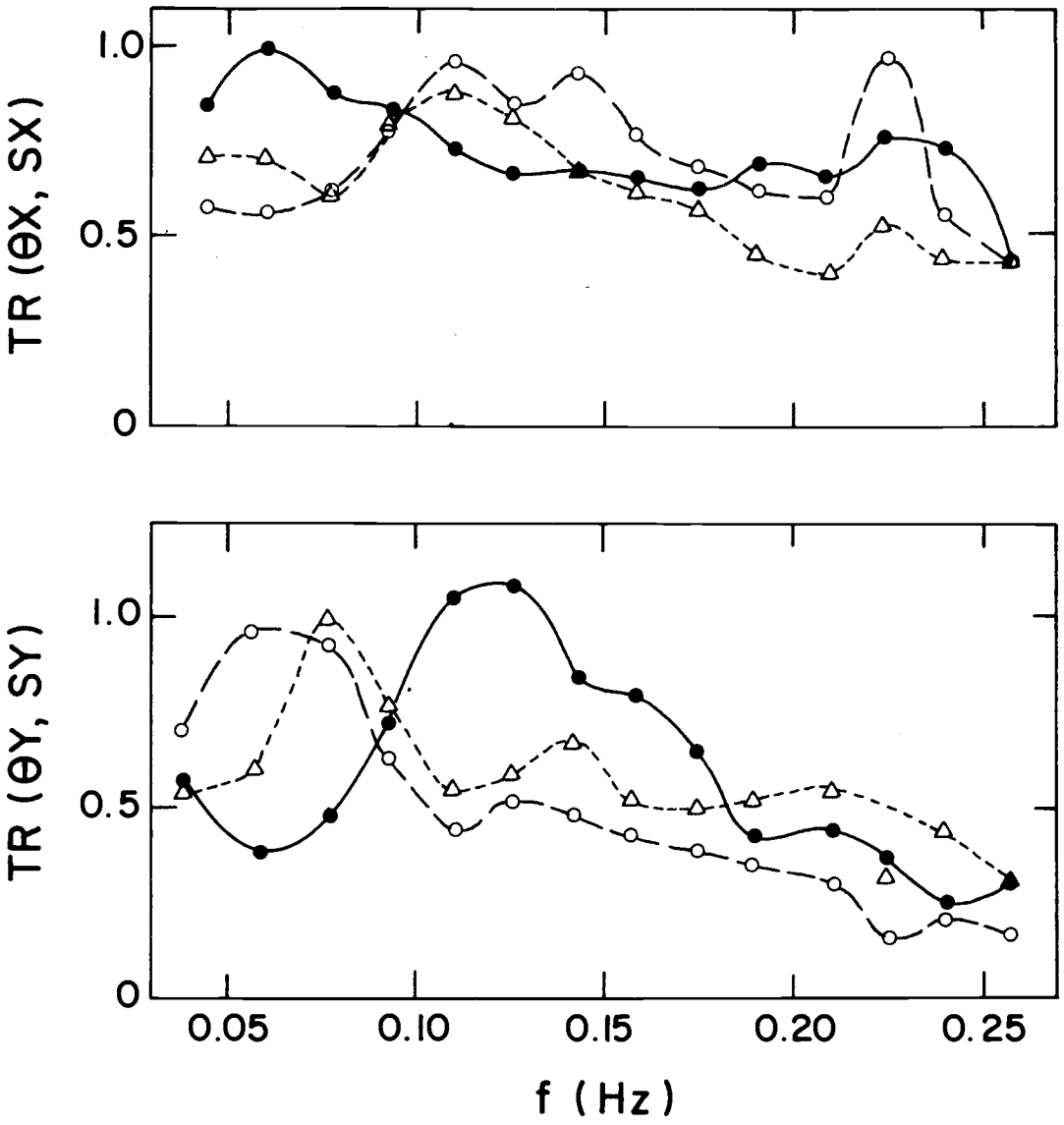

Figure 22. Transfer functions of buoy tilt, X, and wave slope, X (θX, SX) and buoy tilt, Y, and wave slope, Y (θX, SX).

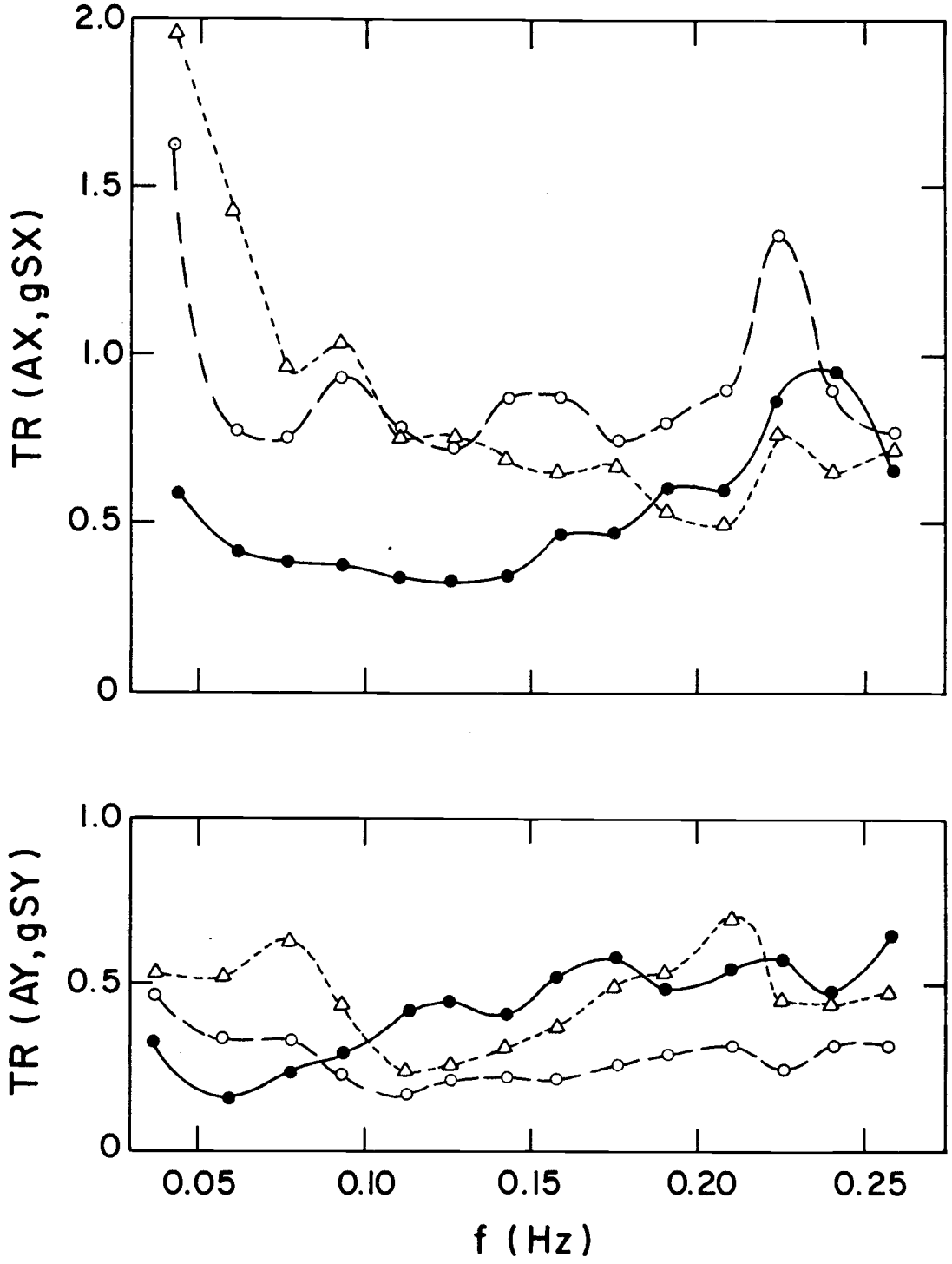

Figure 23. Transfer functions of buoy acceleration, X, and wave slope, X (AX, gSX), and buoy acceleration, Y, and wave slope, Y (AY, gSY).

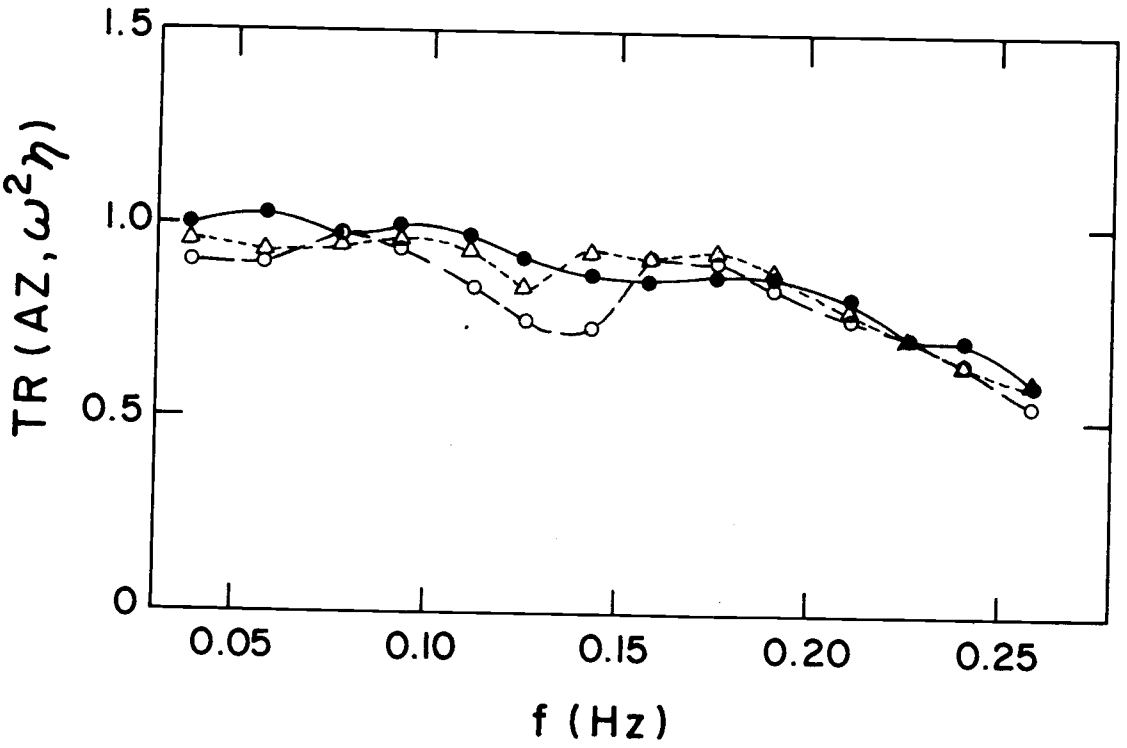

Figure 24. Transfer functions of buoy acceleration, Z, and wave height, η (AZ, $\omega^2 \eta$).

The AX, gSX transfer function is about 0.6 while the AY, gSY transfer function is around 0.3. The buoy damps the horizontal accelerations even more than the torques. In contrast, the AZ, $\omega^2\eta$ transfer function is close to 0.9 in the wave band, which implies that the buoy is almost a perfect surface follower with regard to the surface displacement.

In some frequencies outside of the wave band, the transfer function may appear erratic. However, this result is not significant as there is relatively little energy outside the wave band and coupling relationships are unreliably measured.

VI. CONCLUSIONS

This buoy is a surface follower for swell but it filters out the shorter waves of the sea. It would be suited for experiments where swell following is desired, as in certain air-sea measurements. Furthermore, swell following makes getting on and off the buoy at sea easier, which is important if one needs to make modifications or repairs at sea.

In cases where there is no significant swell, this buoy would filter out most of the wave energy altogether. These cases would be found in sheltered water or lakes. The spectral input of the buoy's motion in some air-sea measurements may be removed without undo difficulty. Since the frequency of the significant energy of the buoy's motion is highly concentrated in a narrow band (between 0.1 to 0.5 Hz) and turbulence spectra have high values over a few decades of frequency, the buoy influenced frequencies would appear as a spike which could be removed. Thus, this small spar buoy is a suitable platform to use in air-sea measurements having the advantages of much less flow interference and motion than a surface ship. Its motion is larger than a platform such as FLIP but its interference with the flow is much less and its motion effects can be removed when necessary.

Tilts are less than the slope of the sea. This buoy should never

experience RMS tilts of more than 10^{o} and thus it would have very little affect on measurements of the Reynold's stress (less than 5%) (Pond, 1968).

BIBLIOGRAPHY

Blackman, R. B. and J. W. Tukey. 1958. The measurement of power spectra. New York, Dover Publications. 190 p.

Bronson, E. D. and L. R. Glosten. 1968. Floating instrument platform. Marine Physical Laboratory, San Diego, California.

Jenkins, G. M. and D. G. Watts. 1968. Spectral analysis and its applications. San Francisco, Holden-Day. 525 p.

Kinsman, B. 1965. Wind waves. Englewood Cliffs, Prentice-Hall, Inc. 676 p.

Lathi, B. P. 1968. An introduction to random signals and communication theory. Scranton, International Textbook Company. 488 p.

Longuet-Higgins, M. S., D. E. Cartweight and N. D. Smith. 1963. Observations of the directional spectrum of sea waves using the motions of a floating buoy. Ocean Wave Spectra. Englewood Cliffs, Prentice-Hall, Inc. p. 111-131.

Pond, S. 1968. Some effects of buoy motion on measurements of wind speed and stress. Journal of Geophysical Research 73(2): 507-512.

Rudnick, P. 1964. FLIP: An oceanographic buoy. Science 146: 1268-1273.

_____ 1967. Motion of a large spar buoy in sea waves. Journal of Ship Research 11(4):257-267.

APPENDICES

APPENDIX I

SYMBOLS AND COORDINATE SYSTEMS

Accelerations

a1	measured horizontal acceleration in direction x
a2	measured horizontal acceleration in direction y
a3	measured vertical acceleration
A1	corrected horizontal acceleration in direction x
A2	corrected horizontal acceleration in direction y
A3	corrected vertical acceleration
AX	horizontal acceleration in stationary direction x
AY	horizontal acceleration in stationary direction y
AZ	vertical acceleration in stationary vertical

Tilts

θX	measured and actual tilt off vertical in x direction
θY	measured and actual tilt off vertical in y direction
ϕ	total tilt of the buoy off vertical

Wave Height

W	measured wave height
η	wave height in stationary system

Wave Slopes

s1	measured wave slope in direction 1
s2	measured wave slope in direction 2
SX	wave slope in xz plane
SY	wave slope in yz plane

APPENDIX II

CALCULATION OF THE RADIUS OF GYRATION

Webster (1929) points out that there are two couples that act on a floating object such as a buoy. The first is a gravity-buoyancy couple and the second is an emersion-immersion couple.

The gravity-buoyancy couple is the significant couple and righting factor for this spar buoy. The center of gravity is 1.56 meters below the center of buoyancy, insuring a strong righting moment. The center of buoyancy is effectively the geometric center of the five submerged toroids that provide the flotation for the buoy. The total couple is:

$$\Gamma = gmr$$

In this case, m = 546 kgms and r = 1.56 meters; the total couple is 8.34×10^{3} kgm m^{2} sec^{-2}.

The top two toroids are responsible for the emersion-immersion couple. When the buoy tilts, part of the "above the surface" toroid is emersed, while part of the "below the surface" toroid is immersed. This causes a slight geometrical change in the arrangement of the displaced water and the result is a righting couple. The emersion-immersion couple is:

$$\Gamma = g\rho v$$

where v is the volume immersed, and r is the distance between the

centers of volume. For a tilt of 5^{o}, the resulting righting couple would be 2.97 kgm m^{2} sec^{-2}. Clearly the emersion-immersion couple is negligible compared to the gravity-buoyancy couple.

The significant righting couple of the buoy is the gravity-center of buoyancy. Therefore the buoy rotates about the center of flotation. The radius of gyration is the distance from the instrument to the center of flotation, which is 4.45 meters.